# ~~Multi-centuries~~Multicentury mean summer temperature variations in the Southern Rhaetian Alps reconstructed from *Larix decidua* blue~~-~~intensity data

Riccardo Cerrato[1], Maria Cristina Salvatore[1, 2], Michele Brunetti[3], Andrea Somma[1], Carlo Baroni[1, 2]

[1]Earth Sciences Department, University of Pisa, Pisa, 56124, Italy
[2]Geosciences and Earth Resources, National Research Council of Italy, Pisa, 56124, Italy
[3]Institute of Atmospheric Sciences and Climate, National Research Council of Italy, Bologna, 40129, Italy

*Correspondence to*: Riccardo Cerrato (riccardo.cerrato@unipi.it)

**Abstract**

Ongoing climate change is likely to cause a worldwide temperature increase of 1.5 °C by the mid-century. To contextualize these changes in a long-term context, historical climatological data extending beyond data obtained from instrumental records are needed. This is even more relevant in remote areas characterized by complex climatic influences and where climate sensitivity is pronounced, such as the European Alps. ~~Dendroclimatology has~~Considering their high temporal resolution, dendrochronological data have been recognized as a fundamental tool for reconstructing past climate variations ~~because its temporal resolution is higher than that of other proxies~~. In this study, we present a comprehensive dendroclimatic analysis in which blue intensity (BI) data derived from European larch (*Larix decidua* Mill.) trees in the Southern Rhaetian Alps were employed. By establishing the relationships between BI patterns in tree rings and climate variables, we explored the possibility of using the obtained data for constructing a high-resolution, long-term climate record ~~is explored~~. The results in the high-frequency domain showed that BI data from European ~~larch share greater variance with~~ larches explained up to 38.4 % (26.7–48.5 %) of the June–August mean ~~temperatures~~ temperature variance in the study area; this result is 70 % greater than the mean temperature variance percentages explained by total ring width measurements~~.~~ for the same period in the area. Moreover, the correlation values between the BI ~~performance as a temperature predictor resulted temporal~~ data and June–August mean temperature are stable over time, ranging between 0.40 and 0.71 (mean value of 0.57), considering a moving window of 50 years, as well as spatial ~~quite stationarity and its~~scale, with significant values over the western and central Mediterranean areas returned for all the considered time windows. In fine, the regression ~~indices are~~ performance using BI data is comparable to ~~those obtainable by~~ that using data from ~~the~~ more expensive ~~wood density method~~methods of analysis. The results from this analysis will extend the current knowledge on the applicability of using BI data to study the European larch, and the reconstruction described herein is the first attempt to determine whether this proxy can be ~~utilized~~used for dendroclimatic aims. Thus, BI data represent a ~~new~~ tool for extending our knowledge beyond that obtained from instrumental records and for facilitating a more robust evaluation of climate models and future climate scenarios.

## 1 Introduction

Climate change has been recognized as unequivocally induced by human activities (IPCC, 2023; Eyring et al., 2023), and it is extremely likely that this activity has been the dominant cause of the observed warming since the mid-20th century (IPCC, 2013). Although human-induced global warming is likely to cause a worldwide temperature increase of 1.5 °C between 2030 and 2050 CE (IPCC, 2018), ~~its~~the effects of global warming on high-altitude areas ~~are even more emphasized, with~~, which have a temperature increase rate that ~~is~~ almost ~~double~~doubles that of the global mean, are even more emphasized (Pepin et al., 2015; Brunetti et al., 2009; Auer et al., 2007; Böhm et al., 2001). This enhanced warming rate implies not only ~~an~~ accelerated glacier melting, reduced snow cover duration, and permafrost thawing but also, as a consequence, disruption of the hydrological cycles, disturbance of terrestrial and freshwater species and ecosystems, slope instability and a greater probability of wildfires ~~(Carrer et al., 2023; IPCC, 2019a).~~(Carrer et al., 2023; IPCC, 2019). Understanding the dynamics of climate variability over centuries has been not only a scientific endeavour but also a pressing concern for society at large, as ~~it provides~~these dynamics provide critical insights into the Earth's response to natural and anthropogenic factors ~~(IPCC, 2023, 2019a, b, 2018).~~(IPCC, 2023, 2022, 2019, 2018). Thus, to contextualize ongoing climate and global changes in a wider frame, precise information on past environmental and climatic conditions is needed.

Long-term and validated meteorological instrumental time series are the best tools for studying and analysing the climate of the past, but these data are not spatially homogeneous and are rarely available for remote sites. Moreover, ~~their~~the time span of these data can also represent a limitation. For instance, the European Alps are among the areas ~~in which~~where long-term meteorological instrumental time series ~~exist, covering~~, which cover at least the last two centuries, exist (Brunetti et al., 2012; Auer et al., 2007; Brunetti et al., 2006). However, the number of meteorological stations, and thus their representativeness of the high-elevation and remote regions in the inner alpine valleys, ~~is much lower~~decreased before 1875 CE (Brunetti et al., 2006). Thus, the use of proxies that cover several centuries and that are capable of representing meteorological variables in recent times is useful for inferring the meteorological conditions that occurred before the beginning of the 19th century ~~is essential for~~, thus permitting a better understanding of the climate changes that ~~involve~~involved high mountain areas since the end of the Little Ice Age.

Among the climatic proxies that can be used (Trachsel et al., 2012), ~~dendrochronology represents~~dendrochronological data represent an excellent tool for reconstructing ~~the~~past climatic variations ~~that occurred in the past.~~. In fact, ~~tree-ring-based~~ dendroclimatology has emerged as a powerful ~~tool~~science useful for reconstructing past climate variability~~, offering~~ and offers a unique perspective on long-term environmental changes at both the hemispherical (Esper et al., 2018; Anchukaitis et al., 2017; Wilson et al., 2016) and regional (Büntgen et al., 2011; Corona et al., 2010; Büntgen et al., 2006) ~~scales~~scale at an annual resolution. However, these large-scale reconstructions ~~are dependent~~depend on local data that are also useful for performing reconstructions at the local scale and thus also highlight local climatic patterns ~~as well~~. In this context, the Alps are an important site, representing a hinge among a continental climate that characterizes central Europe, a Mediterranean climate that characterizes southern Europe, and a more Atlantic climate that is present in the westernmost portions of the European

continent. In this context, the Southern Rhaetian Alps, ~~hosting~~which host the southernmost glaciers of the central Alps, present an intriguing region for dendroclimatic investigations, as demonstrated by previous studies performed in ~~the~~this area ~~(Unterholzner et al., 2024; Cerrato et al., 2023, 2020, 2019a, b, 2018; Coppola et al., 2013, 2012; Leonelli et al., 2011)~~(Unterholzner et al., 2024; Cerrato et al., 2023, 2020, 2019a, b, 2018; Coppola et al., 2013, 2012; Leonelli et al., 2011). Traditionally, dendroclimatic reconstructions have relied on measuring the annual total ring width (TRW) of trees. However, the quest for more robust and high-resolution climate records that are less affected by growth trend problems has led to the exploration of ~~innovative~~other methods, such as maximum wood density (MXD), anatomical traits, and isotopes (Leavitt and Roden, 2022; Björklund et al., 2019). Among these, blue intensity (BI) data have emerged as a promising tool, offering a potential alternative to overcome the costs of MXD analysis (McCarroll et al., 2002) and allowing ~~a greater number of~~more laboratories to perform MXD-like analysis (Reid and Wilson, 2020; Wilson et al., 2017b, 2014). In fact, ~~the~~ BI data, derived from the spectral analysis of tree-ring samples, provide climatic information that is virtually identical to that acquired through MXD in terms of nonlinearity, temperature correlation strength, and autocorrelation (Ljungqvist et al., 2020); these data are a function of the cell wall dimension rather than the TRW or cell wall compound (Björklund et al., 2021). However, even if BI and MXD data are comparable, differences between the proxies could emerge as a function of the intrinsically different resolutions of the two methods (Björklund et al., 2019), as is also underlined by the anatomical MXD ~~(Seftigen et al., 2022; Björklund et al., 2020)~~(Seftigen et al., 2022; Björklund et al., 2020).

Blue intensity, albeit a relatively new methodology, has already been tested on several coniferous species (e.g., Scots Pine (*Pinus sylvestris* L.) in Fennoscandia and Scotland, various *Picea* ssp., *Pinus* ssp., and *Tsuga* ssp. in North America and Europe and other coniferous species in Asia and Oceania (see ~~Reid and Wilson, 2020; Cerrato et al., 2023 for more information).~~Cerrato et al., 2023; Reid and Wilson, 2020 for more information). Nevertheless, in the European Alps, only a few studies have been performed using BI data (Cerrato et al., 2023; Arbellay et al., 2018; Nicolussi et al., 2015; Österreicher et al., 2014), and even fewer have been performed on the European larch. Thus, additional tests are needed (Reid and Wilson, 2020). The European larch (*Larix decidua* Mill.), the dominant tree species in the Southern Rhaetian Alps, is particularly well suited for dendroclimatic investigations due to its sensitivity to environmental conditions and longevity, ~~holding~~thus indicating its great potential for dendroclimatic studies ~~(Cerrato et al., 2018; Coppola et al., 2013, 2012; Büntgen et al., 2011, 2006)~~(Cerrato et al., 2018; Coppola et al., 2013, 2012; Büntgen et al., 2011, 2006). Although this species has been widely studied using both TRW and MXD, the associated BI data were used only for dendroentomological aims (Arbellay et al., 2018), and a dendroclimatic analysis of the BI data from the European larch is still lacking.

~~This paper aims to~~Here, we present ~~a comprehensive~~the first dendroclimatic analysis ~~and climatic reconstructions utilizing~~of European larch BI data from samples collected in the Southern Rhaetian Alps. The methodology, advantages, and limitations of using BI data in the context of climate reconstructions are analysed, and the relationships between BI data and climate variables are examined ~~with the aim of constructing~~to construct a high-resolution, long-term record of climate variability.

## 2 Study area

The study area is located on the Adamello–Presanella and Ortles– –Cevedale massifs (Southeastern Alps, Southern Rhaetian Alps, Marazzi, 2005). The area is characterized by ~~a high number of~~many peaks exceeding 3000 m a.s.l. (e.g., ~~Vióz~~ Mount Vióz – 3645 m; Mount Adamello ~~Mount~~ – 3554 m; and Mount Presanella ~~Mount~~ – 3558 m) and is one of the most glaciated and glacierized areas in the Italian Alps (Salvatore et al., 2015). The sampling stands on Ortles–Cevedale (Bosco Antico – ANBO ~~– on Ortles–Cevedale;~~ –, 46° 19' 57" N 10° 39' 55" E) and Adamello–Presanella massifs (Val di Barco – BARC – 46° 16' 19" N 10° 42' 21" E and Pradach di Val Palù – PALP – ~~on Adamello–Presanella Massif~~46° 16' 10" N 10° 41' 28" E) belong to treeline ecotones and span between 1820 and 2270 m a.s.l. with a general northern exposure (Fig. 1). European larch individuals are scattered in an environment where ericaceous species are predominant (*Rhododendron ferrugineum* L., *Vaccinium* spp.) ~~(Andreis et al., 2005; Gentili et al., 2013, 2020).~~(Gentili et al., 2020, 2013; Andreis et al., 2005). Soils are commonly influenced by parent material and superimposed vegetation and can be classified as immature and shallow podzols, histosols or umbrisols (Galvan et al., 2008; IUSS Working Group, 2007~~; Galvan et al., 2008~~).

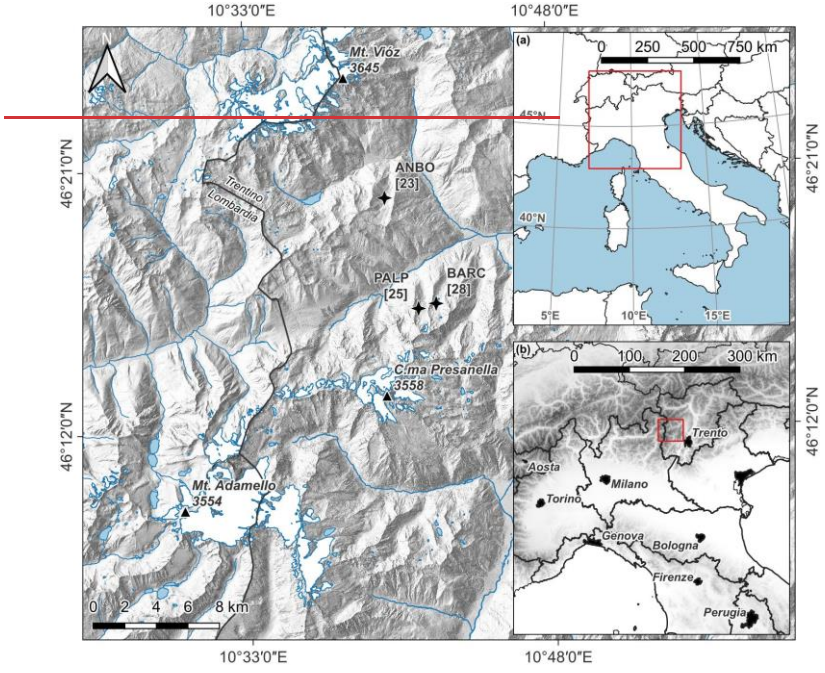

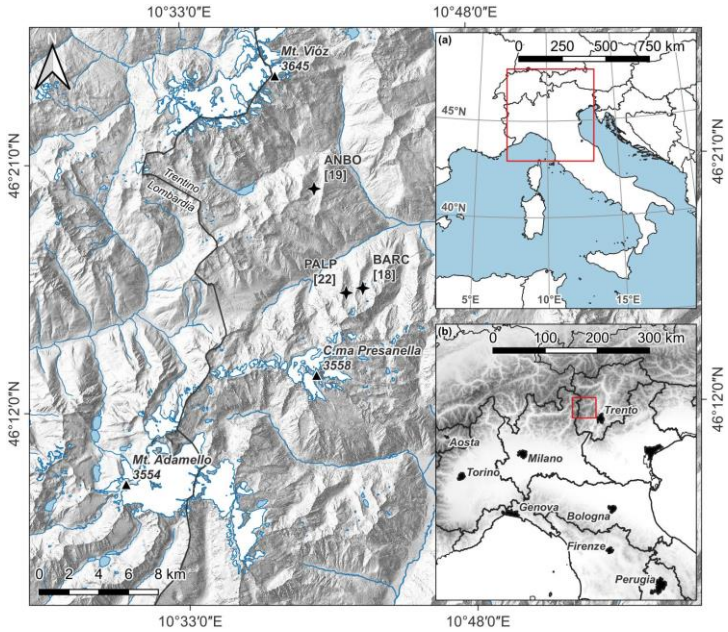


**Figure 1: Map of the study area and sampling sites. ~~Stars~~The stars indicate the sampling sites. ~~Numbers~~The numbers within the square ~~bracket~~brackets indicate ~~sample size~~the number of trees. Inset (b) base map: European Union Digital Elevation Model (EU-DEM). The red squares in insets (a) and (b) represent the footprint of inset (b) and the main map, respectively.**

The area is characterized by a latitudinal precipitation pattern that ~~shows a decreasing trend~~decreases northwards and is located just south of the ~~so-called~~ "inner dry alpine zone" (Isotta et al., 2014). The precipitation distribution reaches a minimum in winter (December–February) and a maximum in summer~~,~~ (June–August) at ~~140.8~~172 mm and ~~288.1~~292 mm, respectively~~,~~; whereas the mean annual value is ~~928.4~~1017 mm in the 1961–1990 period ~~(Crespi et al., 2018; Carturan et al., 2012). Considering the temperature~~(Crespi et al., 2018; Carturan et al., 2012; Brunetti et al., 2006). Considering the temperatures, the 1961–1990 mean annual temperature measured at the nearest station (Careser meteorological station ca. 12 km northwards from the sampling stands and located at 2607 m) was –1.2 °C, with February representing the coldest month (–8.3 °C) and July the warmest month (+6.9 °C).

## 3 Materials and methods

### 3.1 Tree-ring and blue intensity data

In this study, cores from 76 European larch trees were sampled over the past decade and prepared for ~~total ring width (~~TRW~~)~~ measurements (for sampling, sample preparation, measurement, and cross-dating details~~,~~; refer to Cerrato et al. ~~2018, 2019b).~~2019b, 2018). The collected samples were repolished with progressively finer sandpapers with up to P2000 grit to remove pencil marks and to highlight the ring boundaries~~, then they~~. The samples were then scanned at 3200 dpi using ~~a flat-bed scanner~~ an Epson Perfection V850 Pro flatbed scanner (Seiko Epson Corporation, Suwa, Japan) with SilverFast Archive Suite 8 software (LaserSoft Imaging AG, Kiel, Germany). The scanner acquisition colours were calibrated using an IT8.7/2 colour card. BI measurements were subsequently performed using CooRecorder 9.5 Software (Cybis 2020 – http://www.cybis.se/forfun/dendro/index.htm).

The settings of the frame for calculating the BI value can vary depending on the species, site and scientific purpose ~~(Buckley et al., 2018; Dannenberg and Wise, 2016; Schwab et al., 2018; Kaczka et al., 2018; Rydval et al., 2014; Tsvetanov et al., 2020). In this study, a frame width of 100 pixels was used to measure the minimum latewood BI (LWBI) and maximum earlywood BI (EWBI) values, whereas frame depths of 50 and 200 were used for measuring the LWBI and EWBI, respectively. The offset of the frame was set at 5 and −2 for the LWBI and EWBI, respectively (Fig. S1 in the Supplementary Material). For both the LWBI and EWBI, we considered the mean values of the 25 %, 50 %, 75 % and 100 % of the darkest (and lightest when considering the EWBI) pixels in the frame~~(Tsvetanov et al., 2020; Buckley et al., 2018; Kaczka et al., 2018; Schwab et al., 2018; Dannenberg and Wise, 2016; Rydval et al., 2014). In this study, considering that cores with a diameter of 5.15 mm were involved, a frame width of 100 pixels (equal to 0.8 mm at 3200 dpi) was used to measure the minimum latewood BI (LWBI) and maximum earlywood BI (EWBI) values. Frame depths of 50 and 200 pixels (equal to 0.4 and 1.6 mm at 3200 dpi, respectively) were considered good compromises between the average wood structure width and the measurement necessities and were subsequently used for measuring the LWBI and EWBI, respectively. The offset of the frame was set at 5 and –2 pixels for the LWBI and EWBI, respectively (Fig. S1 in the Supplementary Material). For the LWBI measurements, we considered the mean values of the 25 % of the darkest pixels in the frame, whereas all the pixels within the frame were considered for the EWBI measurements (Cerrato et al., 2023). For easier comparison with climate data, BI values were inverted following standard procedures (Rydval et al., 2014; Wilson et al., 2014).

Extractives and wood discolouration are other issues encountered in BI studies that devise different solutions on the basis of species, site, and scientific purpose ~~(Solomina et al., 2016; Fuentes et al., 2018; Sheppard and Wiedenhoeft, 2007; Wilson et al., 2017a). Following Arbellay et al. (2018), in this study, the extractives were not removed; however, to correct the heartwood/sapwood discolouration that characterizes European larch, 16 Delta BI (DBI) datasets were calculated and analysed as differences between the EWBI and LWBI datasets (Björklund et al., 2015, 2014)~~(Fuentes et al., 2018; Wilson et al., 2017a; Solomina et al., 2016; Sheppard and Wiedenhoeft, 2007). Following the procedure applied to the European larch (Arbellay et al., 2018) and other conifer species (Wilson et al., 2021, 2019, 2014), in this study, the extractives were not removed; however,

to correct the heartwood/sapwood discolouration that characterizes this species, Delta BI (DBI) datasets were calculated as differences between the LWBI and EWBI datasets and analysed (Björklund et al., 2015, 2014).

The obtained BI ~~sample series were visually and statistically cross-dated with the TRW series to check the correctness of the results. BI sample series belonging to the same individual were averaged to create the individual BI series. Some individual BI series showed an age trend; thus, they were standardized using a modified negative exponential curve. If the modified negative exponential curve failed to fit the trend of the individual series, they were standardized using a negative or a horizontal line. Following the first standardization, to highlight the high-frequency domain (*sensu* Melvin 2004) and attenuate the discolouration bias in EWBI and LWBI, a high-pass Gaussian filter with a window length of 30 years and a sigma of 5 years was applied to the individual series. The mid-low-frequency domain was obtained using the same filter as a low-pass filter. Only those series that showed high correlation values with the site master chronology (i.e., p-value less than 0.001 and Spearman's ρ greater than or equal to 0.30) were considered to construct the site chronologies.~~

~~Site chronologies were obtained as a biweighted robust mean of the~~core series were visually and statistically cross-dated with the TRW core series to check the correctness of the results. Due to the occurrence of Larch Budmoth outbreaks (*Zeiraphera diniana* Gn.; LBM) in the area (Cerrato et al., 2019b; Turchin et al., 2003; Baltensweiler and Rubli, 1999), the BI core series were checked and corrected via the gap filling procedure (Büntgen et al., 2006). After LBM correction, the BI core series belonging to the same tree were averaged to create the individual BI tree series. Then, individual BI tree series were standardized using a modified negative exponential curve or a linear regression (Cook and Holmes, 1999). Site chronologies were obtained as a biweighted robust mean of the individual BI tree series belonging to each site where the variance was stabilized as a function of the sample depth (Schweingruber, 1988; Fritts, 1976). Only those individual BI tree series that showed high correlation values with the site chronology (i.e., p values less than 0.001 and Spearman's ρs greater than or equal to 0.30) were considered. The expressed population signal (EPS) was calculated to estimate the representativeness of ~~the sampling~~each chronology compared to an infinite hypothetical population~~, considering the uneven sample depth~~ (Fritts, 1976), and the commonly used threshold of 0.85 was used to limit the site chronologies in time. Finally, to highlight the mid-low-frequency domain (*sensu* Melvin 2004), a low-pass Gaussian filter with a window length of 30 years and a sigma of 5 years was applied to the BI site chronologies. The high-frequency domain of the site chronologies was obtained as residuals of the raw data from the low-pass filter.

To highlight the common signals that characterize the three site chronologies, principal component analysis (PCA) and evolutionary principal component analysis (EPCA) were performed on the raw data and on the low- and high-frequency domains (Camiz and Spada, 2023; Camiz et al., 2020). This approach limits the period of analysis to the shortest considered site chronology but allows the retention of only those factors that explain the *a priori* decided quantity of the original data variance. In this study, the components that explained 80 % of the variance in the original dataset were considered.

All the data were manipulated in the R-project environment ~~(R Core Team, 2022)~~(R Core Team, 2024) by using dplR ~~(Bunn, 2008, 2010)~~(Bunn, 2010, 2008) and smoother (v. 1.1, https://CRAN.R-project.org/package=smoother, accessed on 09 October

2023) packages, whereas ~~the~~ principal component analysis was performed using the 'stat' and FactoMineR (Lê et al., 2008) packages.

### 3.2 Instrumental data

Instrumental series for minimum, maximum and mean temperature and for precipitation were considered to explore the sensitivity of the BI chronologies to climate variability. Meteorological series from 1764 to 2015 specific to the sampling stands were reconstructed by interpolating the climate information provided by meteorological station data by using the anomaly method (Mitchell and Jones, 2005; New et al., 2000) and interpolating the longest and homogenized meteorological series available for the Alpine region (Crespi et al., 2021, 2018; Brunetti et al., 2014, 2012, 2006). The interpolation procedure consists of the independent reconstruction of the climatologies (i.e., the climate normals over a given reference period) and the deviations from them (i.e., anomalies). Climatologies, linked to geographic features of the territory, are characterized by large spatial gradients; anomalies, linked to climate variability and change, are generally characterized by greater spatial coherence than climate normals. Therefore, the former were reconstructed by applying an interpolation technique that exploits the local dependence of meteorological variables on elevation (Crespi et al., 2018; Brunetti et al., 2014). This technique requires a high spatial density station network, even if the data are available for a limited period only. On the other hand, anomalies can be reconstructed through a simpler interpolation technique and a lower station density. However, long temporal coverage is mandatory, as is accurate homogenization of the time series for removing nonclimatic signals (e.g., due to instrument relocation and changes in measurement practices). Finally, from the superimposition of climatologies and anomalies, monthly temperature and precipitation series in absolute values that were representative of the specific sites were obtained.~~Meteorological series from 1764 to 2015 specific to the sampling stands were reconstructed by interpolating the climate information provided by meteorological station data using the anomaly method (New et al., 2000; Mitchell and Jones, 2005) and interpolating the longest and homogenized meteorological series available for the Alpine region (Brunetti et al., 2006, 2012, 2014; Crespi et al., 2018)~~ Information about the techniques and their accuracy is provided in Brunetti et al. (2014, 2012) and Crespi et al. (2021, 2018). All the information concerning the meteorological stations involved in the climate information reconstruction is summarized in Fig. S2 (in the Supplementary Material), which shows the spatial distribution of temperature and precipitation stations around the sites (Fig. S2a and S2b), the temporal evolution of data availability for those stations located within a radius of 150 km from the centroid of the three sites (Fig. S2c) and their elevation distribution (Fig. S2d~~. The interpolation procedure consists of the independent reconstruction of the climatologies (i.e., the climate normals over a given reference period) and the deviations from them (i.e., anomalies~~).

In addition, to assess the spatial coherence of the dendroclimatic signal, high-resolution (0.5×0.5 degree lat-lon) monthly spatially continuous interpolated gridded datasets of minimum, maximum, mean temperature, and precipitation were used (Harris et al., 2020; Climate Research Unit Time-Series (CRU-TS), v. 4.07; last accessed 10 October 2023). The meteorological data were filtered as BI data to minimize bias in correlation with the tree-ring data resulting from unfiltered trends (Ols et al., 2023; Seftigen et al., 2020; Cerrato et al., 2019a, 2018)

~~Climatologies, linked to geographic features of the territory, are characterized by large spatial gradients; anomalies, linked to climate variability and change, are generally characterized by greater spatial coherence than climate normals.~~

~~Therefore, the former were reconstructed by applying an interpolation technique that exploits the local dependence of meteorological variables on elevation (Brunetti et al., 2014; Crespi et al., 2018). This technique requires a high spatial density station network, even if the data are available for a limited period only.~~

~~On the other hand, anomalies can be reconstructed through a simpler interpolation technique and a lower station density. However, long temporal coverage is mandatory, as is accurate homogenization of the time series for removing nonclimatic signals (e.g., due to instrument relocation and changes in measurement practices).~~

~~Finally, from the superimposition of climatologies and anomalies, monthly temperature and precipitation series in absolute values that were representative of the specific sites were obtained.~~

~~Information about the techniques and their accuracy are provided in Brunetti et al. 2012, 2014 and Crespi et al. 2018.~~

~~In addition to the site-specific series reconstructed as described above, the Climatic Research Unit (CRU) time series (TS) version 4.07 of a high-resolution spatially continuous interpolated gridded dataset (Harris et al., 2020) was accessed through the CEDA archive (https://data.ceda.ac.uk/badc/cru/data/cru_ts/cru_ts_4.07, last accessed 10 October 2023) to assess the spatial coherence of the dendroclimatic signal. The meteorological data were filtered as BI data to minimize bias in correlation with the tree-ring data resulting from unfiltered trends (Cerrato et al., 2018, 2019a; Seftigen et al., 2020; Ols et al., 2023)~~

### 3.3 Climate correlation and reconstruction

The BI–climate relationship was assessed by calculating Pearson's correlation indices between the BI chronologies and climatic parameters. The correlation indices were calculated over the ~~1764~~1800–2013 period while considering the monthly values from the previous May to October or the current year of growth~~,~~ for a total of 18 months. In addition, considering the climatic sensitivity of the European larches in the area ~~(Coppola et al., 2013; Cerrato et al., 2018), seasonal variables were created and examined by averaging the temperature of the June–August (JJA) period. The stability of the BI–climate relationship over time was verified through moving correlation analysis performed for each year using a window width of 50 years. Correlation indices were calculated in the R-project statistical environment by means of~~(Cerrato et al., 2018; Coppola et al., 2013), seasonal variables were created and examined by averaging the climatic parameter over the June–August (JJA) period. Using a window width of 50 years, the stability of the BI–climate relationship over time was verified by performing a moving correlation analysis with a 1-year step. Correlation indices were calculated in the R-project statistical environment via the treeclim (Zang and Biondi, 2015) package ~~applying the~~. The bootstrapping procedure described in DENDROCLIM2002 ~~(Biondi and Waikul, 2004)~~(Biondi and Waikul, 2004) was applied to calculate the correlation indices and their 95 % confidence intervals via the percentile confidence interval method (Zang and Biondi, 2015; Dixon, 2001).

To test the stationarity of the transfer function and thus to assess the reliability of the reconstruction (Wilmking et al., 2020), a bootstrapped cross-calibration-verification (CCV) approach was applied, and the reduction in error (RE) and the coefficient of efficiency (CE) were calculated ~~(Fritts, 1976; Cook et al., 1994).~~(Cook et al., 1994; Fritts, 1976). Moreover, the bootstrapped

transfer function stability test (BTFS) was performed (Buras et al., 2017). The process was repeated 1000 times. Dendroclimatic reconstruction was assessed by performing linear regression between z-scores of both BI values (predictor) and meteorological data (predictand) while considering an ordinary least-square regression approach. Then, the mean and the variance of the DBI data were adjusted against the instrumental targets to avoid the typical loss of amplitude due to regression error (Carrer et al., 2023).

## 4 Results

Seventeen of the 76 individual BI tree series from the three sampled stands were excluded from the study because they exhibited low interseries correlation values. From the other 59 individual BI tree series, considering the EPS, the BI values of 18931 rings spanning 514 years (i.e., 1502–2015 CE; Table 1) were obtained. From each site, the EWBI, LWBI and DBI site chronologies were obtained. The EWBI and LWBI site chronologies showed the influence of wood discolouration at the most recent end (Fig. S3 in the Supplementary Material), whereas DBI chronologies did not show an evident influence of discolouration due to the heartwood-sapwood transition (Fig. 2).

Table 1: Statistical parameters of the BI chronologies and their Pearson's ($\bar{r}$) and Spearman's ($\bar{\rho}$) mean interseries correlation coefficients. ~~From the 76 sampled trees, 24 BI series (i.e., four EWBI, four LWBI and 16 DBI series) of 24248 rings were obtained for a maximum period of 599 years (i.e., 1418–2016 CE; Table 1). Considering the EPS, the remaining chronologies spanned between 1502 and 2015 CE for a total of 514 years, whereas the mean interseries correlation increased by 0.05 at most (Pearson's $\bar{r}$, Table 1).~~

**The correlation index between chronologies was calculated considering the raw chronologies on the maximum overlap considering the EPS. *EPS identify values for the EPS-stripped chronology as described in Sect. 3.1.**

| ~~valley~~Chronology code | Time span ~~[total years]~~ [*EPS~~* span ~~[total years~~] | Length [*EPS] | ~~n~~N. of trees ~~[used]~~ | $\bar{r}$ ~~[~~ [*EPS~~*~~ $\bar{r}$] $\bar{\rho}$ ~~[EPS* $\bar{\rho}$]~~ | $\bar{\rho}$ [*EPS $\bar{\rho}$] | ~~correlation~~Correlation with other chronologies |
|---|---|---|---|---|---|---|
| ANBO | 1418–2015 ~~[598]~~ [1502–2015 ~~[514~~] | 598 [514] | ~~23 [~~19~~]~~ | 0.51 [0.54] ~~0.50 [0.53]~~ | 0.50 [0.53] | BARC: 0.68 PALP: 0.70 |
| BARC | 1502–2016 ~~[515]~~ | 515 [284] | ~~28 [~~18~~]~~ | 0.43 [0.45] | ~~0.43 [0.45]~~ 0.40 | PALP: 0.77 – |

| | | | | | |
|---|---|---|---|---|---|
| | [1730–2013 | | | | [0.40] |
| | ~~[284]~~ | | | | |
| PALP | 1566–2015 | 450 | ~~25 [22]~~ | 0.49 | 0.51 |
| | ~~[450]~~ | [405] | | ~~[0.54]~~ | [0.54]~~–~~ |
| | [1611–2015 | | | ~~0.51~~ | – |
| | ~~[405]~~ | | | [0.54] | |
| ~~*PC*~~*APC1* | *1730–2013* | *284* | ~~*76 [59]*~~ | | |
| *(ANBO+BARC+PALP)* | ~~*[284]*~~ | *405* | ~~*48 [41]*~~ | | |
| ~~*PC*~~*APC1 (ANBO+PALP)* | *1611–2015* | | | | |
| | ~~*[405]*~~ | | | | |

~~**Table 1: Statistical parameters of the resulting BI chronologies and their Pearson (*r*) and Spearman ($\bar{\rho}$) mean interseries correlation coefficients. *EPS stripped chronology as described in Sect. 3.1.**~~

The ~~analysis of the 24 BI chronologies and their correlation with meteorological datasets revealed that the influence of the considered percentage of the LWBI darkest pixels, as well as that of the EWBI lightest pixels, slightly affected the results. However, in general,~~three DBI ~~values obtained from a small percentage of the darkest LWBI pixels (i.e., 25 %) and from a large percentage of the EWBI pixels (i.e., 100 %) yielded better results considering the values of their correlation with meteorological data (not shown). Thus, for further analysis, the series obtained from the difference between 25 % of the darkest latewood pixels BI and 100 % of the earlywood pixels BI were used and identified as DBI.~~

~~The DBI site~~ chronologies showed ~~a~~ similar ~~trend~~decadal variabilities, with only ~~the~~ BARC reporting a slightly positive ~~upwards~~ trend over time (Fig. 2). ~~Moreover, the maximum sample depth of each chronology was comparable in quantity but not in time, with the duration reduced by approximately 100 years between ANBO and PALP and another 100 years between PALP and BARC.~~ Due to the coherence shown by the DBI chronologies, a PCA was performed ~~considering all the chronologies~~ to ~~better preserve~~highlight the common patterns of variability~~, likely related~~ and to evaluate their relationships with climate (Seftigen et al., 2020). ~~Moreover, the use of PCA permits us to obtain a slightly better correlation coefficient when correlated with meteorological time series (not shown).~~

~~The PCA confirmed that the considered chronologies shared a large portion of the original variance. In fact,~~The results showed that the first principal component (PC1) explained more than 80 % of the variance alone, and all the chronologies were strongly positively correlated with PC1 (see Fig. S4 in the Supplementary Material for further details). However, the correlation values obtained between the mean temperature and both the EWBI and LWBI PC1 (ANBO+BARC+PALP) corroborate the hypothesis that the discolouration due to the heartwood-sapwood transition affects the analysis (Fig. S5 in the Supplementary Material), whereas the DBI PC1 (ANBO+BARC+PALP) seems to not be affected by this issue (compare Fig. 3 and Fig. S5 in the Supplementary Material). ~~it. Thus, PC1 (ANBO+BARC+PALP) was selected to represent the areal chronology (Fig. S2 in the Supplementary Material for further details).~~Moreover, comparing the correlation coefficient obtained between the mean

Celle inserite

temperature and both DBI PC1 (ANBO+BARC+PALP) and site DBI chronologies shows that the former returned slightly greater values (Fig. S6 in the Supplementary Material). Thus, the DBI PC1 (ANBO+BARC+PALP), identified here as PC1 (ANBO+BARC+PALP), was selected to represent the mean areal chronology and was used for further analysis.

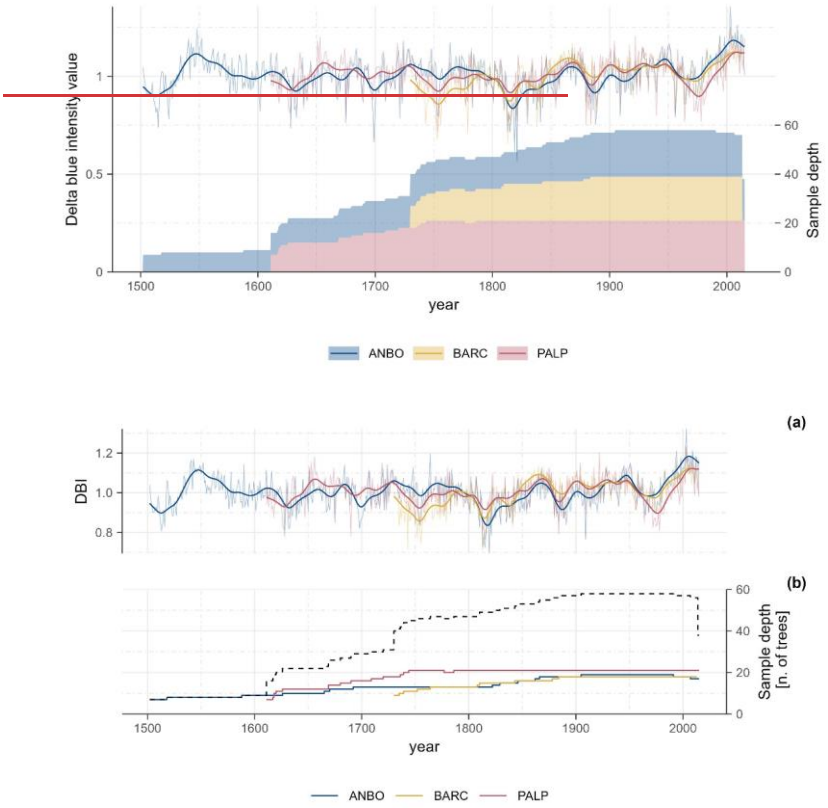


**Figure 2: ~~Delta~~Raw delta blue intensity (DBI) chronologies (a) and sample depths. (b). The thick solid lines in (a) represent 30-year Gaussian-filtered chronologies (σ = 5 years~~).~~); the black dashed line in (b) represents the cumulative sample depth.**

### 4.1 BI–climatic correlations

Concerning the meteorological variables, PC1 (ANBO+BARC+PALP) ~~was correlated with the meteorological datasets. Higher correlation values were obtained with the mean temperatures~~ correlates significantly with temperature (Fig. 3), ~~whereas~~

~~the~~correlates more with mean temperature than with minimum and maximum ~~temperatures returned similar but lower values (~~temperature, and does not ~~shown). Precipitation was also tested, but~~ correlate with precipitation (Fig. S7 in the Supplementary Material). On both the raw data and low- and high-frequency domains, correlations were ~~not significant.~~

~~Regarding the static correlation~~evaluated over the whole period and on moving time windows (see section 3.1 for the definition of high- and low-frequency series).

The correlations of the raw data estimated over the whole period (Fig. 3a~~), PC1 (ANBO+BARC+PALP) exhibited~~ ) show significant positive ~~correlation values~~correlations with ~~temperature~~the temperatures of the previous summer and fall ~~seasons~~ (i.e., May–November of the previous year) and with those of the current late spring and summer ~~seasons~~ (i.e., May–September~~),~~ of the current year). The correlations with the ~~former returning lower~~current spring and summer temperatures returned higher values than ~~did the latter. The highest~~ the correlations with the previous summer and fall temperatures; the correlation with the mean temperature of JJA returned the highest value~~, however, was obtained with the mean temperature during JJA~~ (0.~~68~~71, 95 % confidence interval: [0.~~58~~62–0.~~75). Regarding~~78], Table S1 in Supplementary material). In the low-frequency domain, the correlation was always significant and positive, with the highest values occurring in the summer (~~June–August), both~~JJA) of the current year (0.77, [0.70–0.82]) and with the summer of the previous ~~and current. Even in~~year. Finally, for the ~~low~~high-frequency domain, the highest correlation value was obtained ~~for~~with the mean temperature of JJA of the current ~~JJA~~year (0.~~78, 62~~, [0.~~71~~52–0.~~83). For the~~70]).

The moving window analysis between PC1 (ANBO+BARC+PALP) and the JJA mean temperature revealed correlation values characterized by evident nonstationarity in the low-frequency domain, especially in the 1880s–1930s and 1960s–1980s. However, the correlation coefficients are significant and stable at the 0.01 level when the raw data and high-frequency domain~~, lower values than those of the raw and low-frequency domains were obtained.~~ are considered (Fig. 3b). The correlation ~~was slightly~~ values of the high-frequency domain, beyond their decadal variability, showed a general negative trend (Mann–Kendall S: –4124, p value < 0.001, reference period: 1800–2013). However, after a minimum was observed in the 1921–1970 window, a significant ~~for the previous October (α<0.05) and~~ upwards trend was appreciable (Mann–Kendall S: 728, p value < 0.001 on the windows ending in the 1971–2013 period; Fig. 3b). The high correlation values between PC1 (ANBO+BARC+PALP) and the JJA mean temperature over the examined period are also evident from the comparison of the two temporal series in Fig. 3c for the ~~current summer (June–August). Like in previous~~ raw, high- and low-frequency domains, ~~at high frequencies,~~with the ~~highest correlation results were also obtained for~~BI explaining between 38 % and 59 % of the ~~mean~~ temperature ~~during JJA (0.56, 0.45–0.66~~variance, depending on the considered frequency domain (Fig. 3c).

~~Regarding~~To highlight the ~~moving~~spatial representativeness of our reconstruction, the spatial correlation ~~values obtained~~ between the raw data PC1 (ANBO+BARC+PALP) and JJA mean temperature ~~and both the raw data and high-frequency domains (Fig. 3b), a high degree of stationarity can be observed. In fact,~~was estimated over the ~~correlations are characterized~~Euro-Mediterranean domain by ~~high and stable coefficients (always α<0.01 but α<0.001 for most of~~exploiting the ~~considered windows). Moreover, the raw~~CRU-TS v. 4.07 data ~~did not~~(see section 3.2). The results show a ~~statistically~~ positive and significant ~~trend, in contrast to the high-frequency domain, which is characterized by a negative trend in~~

correlation ~~coefficients (Mann-Kendall S: 7705, p-value<0.001) associated with an increase in variance. Moreover, both correlation series showed a decreasing step in the right-aligned 1964 CE window. In contrast to the raw data and high-frequency domain, the low-frequency domain exhibited greater instability, especially in the 1880s–1930s and 1960s–1980s periods, but with generally more limited variance.~~

~~The high correlation values obtained between PC1 (ANBO+BARC+PALP) and the JJA mean temperature were also corroborated by good visual agreement between the time series and generally high statistics, with BI values that can explain between 31 % and 61 % of the temperature variance as a function of the considered domain (Fig. 3c).~~

~~The spatial correlation between the raw BI and JJA mean temperature data returned positive values which significantly covered all central and southern~~over Central and Southern Europe, North Africa, and the Middle East (p value < 0.001; Fig. 4a). However, the spatial correlation is not stable over time. In fact, after an initial decrease ~~(until~~that limited the ~~1965 CE window), high and~~ significant correlation values ~~were concentrated~~to the areas around the Mediterranean basin until the beginning of the ~~2000s. Since then~~1990s, a strong and rapid increase ~~in the raw spatial correlation~~ was observed (Fig. ~~S3~~S8 in the Supplementary Material).

Considering the ~~spatial representativeness of the~~ high-frequency domain, ~~it was more limited than the raw data but still strongly and positively correlated with a large portion~~significant correlation values were observed over much of the western and central Mediterranean basin (i.e., from ~~20~~15° W to 25° E) ~~to central~~and from Northwestern Africa to Central Europe (~~circa~~i.e., from 23° to 53° N~~)~~ ~~(~~; Fig. 4b). Regarding ~~the~~their stability over time, significant values decreased from ~~an area well established across~~ the central and western Mediterranean and Europe (1955 CE window) to an area that involved mainly Italy, the western Mediterranean, and Algeria in the 2010s (Fig. ~~S4~~S9 in the Supplementary Material).

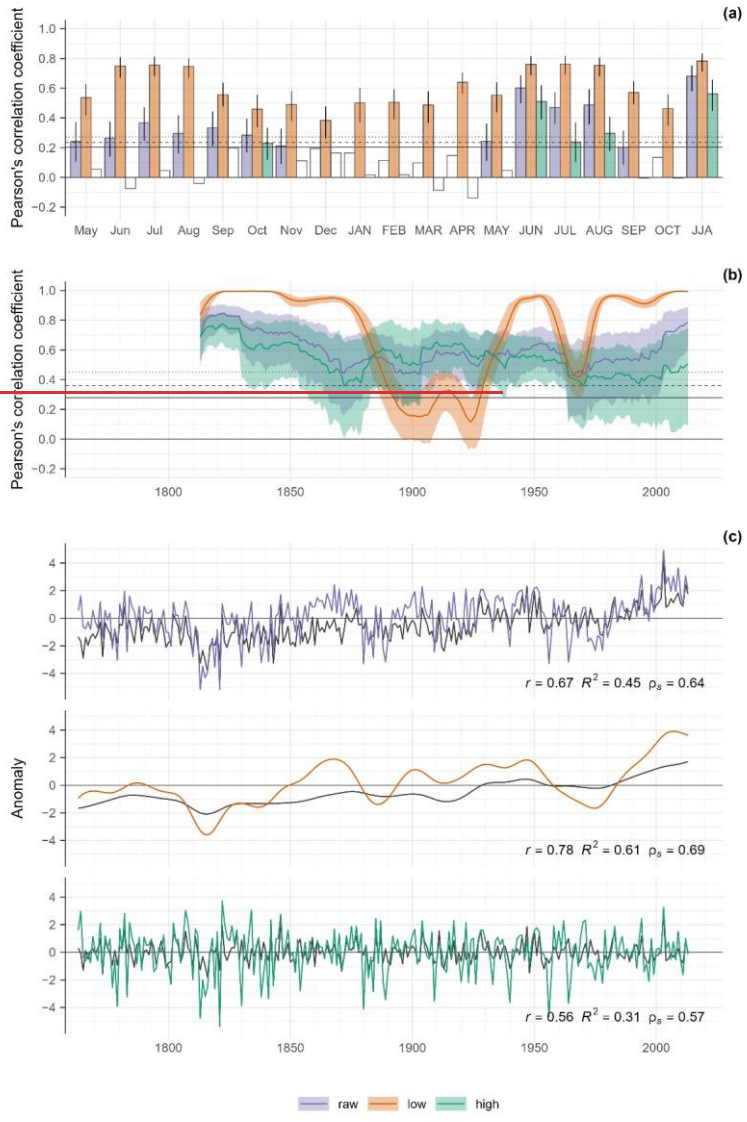
(a)
Pearson's correlation coefficient
1.0
0.8
0.6
0.4
0.2
0.0
−0.2
May Jun Jul Aug Sep Oct Nov Dec JAN FEB MAR APR MAY JUN JUL AUG SEP OCT JJA
(b)
Pearson's correlation coefficient
1800 1850 1900 1950 2000
(c)
Anomaly
r = 0.67 R² = 0.45 ρs = 0.64
r = 0.78 R² = 0.61 ρs = 0.69
r = 0.56 R² = 0.31 ρs = 0.57
raw low high

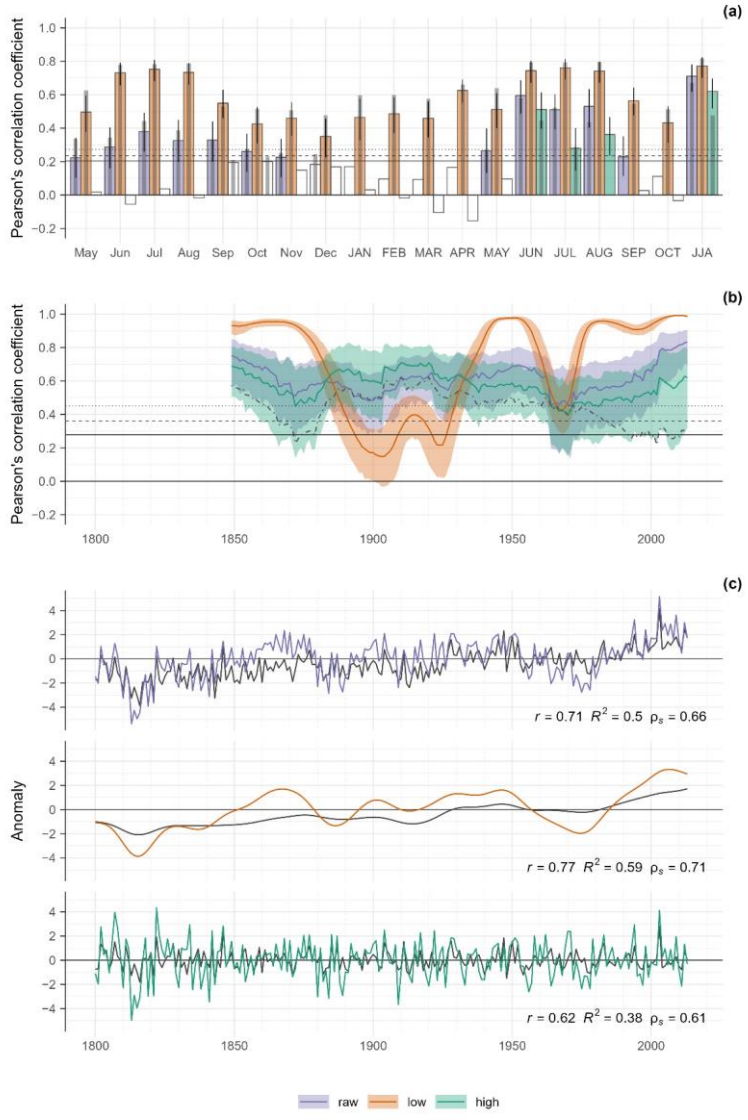
(a)
Pearson's correlation coefficient
1.0
0.8
0.6
0.4
0.2
0.0
−0.2
May Jun Jul Aug Sep Oct Nov Dec JAN FEB MAR APR MAY JUN JUL AUG SEP OCT JJA
(b)
Pearson's correlation coefficient
1800 1850 1900 1950 2000
(c)
Anomaly
r = 0.71 R² = 0.5 ρs = 0.66
r = 0.77 R² = 0.59 ρs = 0.71
r = 0.62 R² = 0.38 ρs = 0.61
raw low high

**Figure 3: Pearson's ~~static~~ correlation coefficient between ~~DBI~~ PC1 (ANBO+BARC+PALP) and the mean temperature for the period ~~1775~~of 1800–2013. The coloured (BI) and dark grey shaded (TRW) bars indicate that the correlation values are significant at least at the 0.05 level. The solid black vertical line indicates the 95 % confidence interval~~. of the BI correlations. All capitalized month abbreviations indicate the current year (a). Pearson's moving correlation coefficient (50-year window, 1-year step, right aligned) between ~~DBI~~ PC1 (ANBO+BARC+PALP) and the JJA mean temperature. The shaded area ~~identifies~~represents the 95 % confidence interval ~~at 95 %~~. The dot-dashed dark grey line refers to the TRW moving correlation in the high-frequency domain for comparison (b). ~~DBI~~ PC1 (ANBO+BARC+PALP) and JJA mean temperature anomalies (grey line) and their ~~Pearson~~Pearson's correlation coefficient ($r$), explained variance ($R^2$), and ~~Spearman~~Spearman's correlation coefficient ($\rho_s$) (c). The solid, dashed and dotted black lines in (a) and (b) represent significance at the 0.05, 0.01 and 0.001 levels, respectively. (For interpretation of the references to colour in this figure legend, the reader is referred to the web version of this article.)**

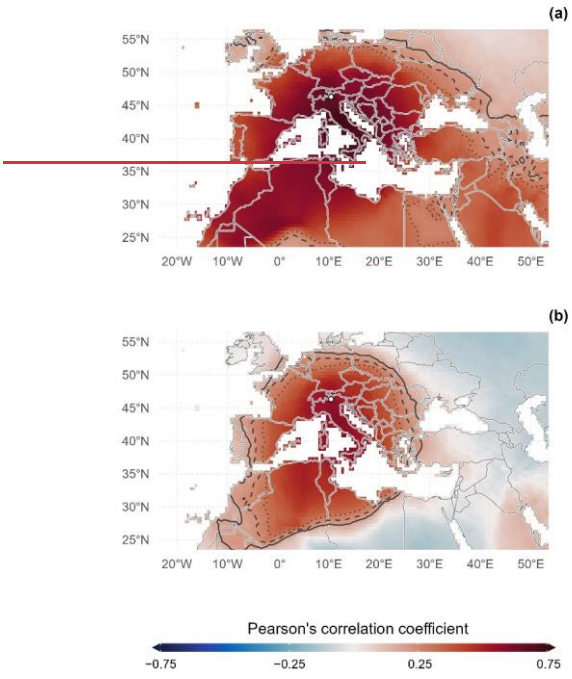

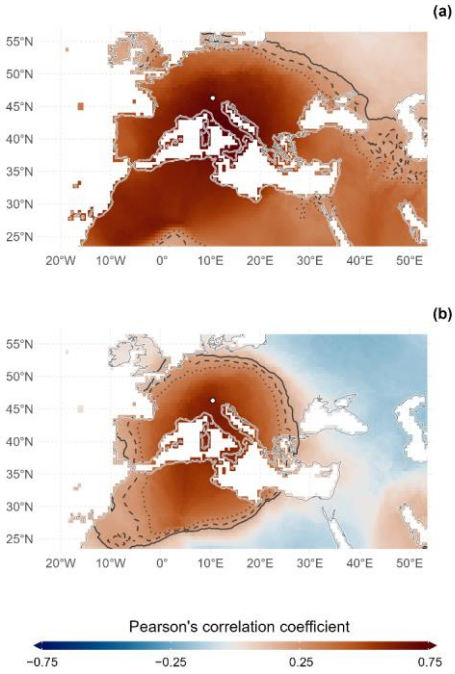


**Figure 4: Pearson's spatial correlation coefficient between ~~DBI~~ PC1 (ANBO+BARC+PALP) and the CRU TS4.07 mean aggregated JJA temperature for the period 1901–2013 for the raw series (a) and high-frequency domain (b). The solid, dashed and dotted black lines represent significance levels of 0.05, 0.01 and 0.001, respectively. The white dots represent the locations of the sampling stands. (For interpretation of the references to colour in this figure legend, the reader is referred to the web version of this article.)**

### 4.2 Mean June–August temperature reconstruction

~~Starting from PC1 (ANBO+BARC+PALP), DBI based~~Based on the above-described results, JJA temperature reconstruction was attempted~~.~~ starting from DBI PC1 (ANBO+BARC+PALP). The transfer function was tested using both the CCV and BTFS approaches, which returned stable results in the high-frequency domain, whereas ~~the instability~~nonstationarity of the transfer function was highlighted for the ~~row~~raw data and low-frequency domain (Table 2). ~~The~~ Considering the CCV results, the amount of explained ~~variances are~~variance was similar ~~in~~for both 1800–1906 and 1907–2013 as the calibration ~~periods used, as are~~period. The same was true for the RE ~~values~~coefficients, which returned positive values with ~~a~~ limited standard ~~deviation~~deviations. In contrast, the CE values were positive only for the high-frequency domain. The CCV results were

corroborated by the results obtained by the more rigorous BTSF tests. Excluding the low-frequency domain, only in one case (i.e., the raw data intercept ratio) did the calculated 95 % confidence interval at 95 % fail to pass the test, thus indicating a difference in offset between the two considered calibration periods (i.e., calibration and validation). Similar results were also obtained for DBI PC1 (ANBO+PALP) (Table S1 in the Supplementary Material). Theand DBI ANBO chronology-based reconstruction, however, failed to pass the BTFS test for the slope ratio and explained variance ratio (Tablereconstructions (Tables S2 and S3 in the Supplementary Material). Finally, the Durbin–Watson test returned significant results for the low-frequency domain and for the regression that used the more recent half of the raw data, as the calibration period, thus highlighting a nonzero autocorrelation in the residuals of these models.

| | Cal. period [CE] | $R^2_{cal}$* | DW | CCV* RE | CCV* CE | BTFS‡ Intercept ratio | BTFS‡ Slope ratio | BTFS‡ $R^2$ ratio |
|---|---|---|---|---|---|---|---|---|
| Raw | 1764–1888 | 0.42±0.08 | 1.71 | 0.42±0.01 | *0.23±0.11* | *[0.888÷0.932]* | [0.584÷1.245] | [0.620÷1.922] |
| | 1889–2013 | 0.39±0.08 | *1.22* | 0.37±0.01 | *0.28±0.16* | | | |
| Low | 1764–1888 | 0.64±0.06 | *0.04* | 0.63±0.01 | *0.69±0.10* | *[0.905÷0.933]* | *[0.575÷0.866]* | [0.949÷1.732] |
| | 1889–2013 | 0.50±0.06 | *0.01* | 0.49±0.01 | *1.92±0.50* | | | |
| High | 1764–1888 | 0.37±0.08 | 2.13 | 0.35±0.01 | 0.23±0.01 | [–8.707÷13.395] | [0.662÷1.845] | [0.672÷3.592] |
| | 1889–2013 | 0.25±0.07 | 2.18 | 0.23±0.02 | 0.34±0.02 | | | |

**Table 2: Explained variances of the calibration periods and statistical parameters of the CVVCCV and BTFS procedures between PC1 (ANBO+BARC+PALP) and the JJA mean temperature. Italicized values identify parameters that do not pass the statistical tests (at the 95 % level, when applicable). *One standard deviation is reported as a measure of uncertainty. ‡95 % confidence†Confidence intervals at 95 % are reported for BTSF parameters. For a detailed description of the BTFS parameters, please refer to Buras et al. 2017.**

Regarding the PC1 (ANBO+BARC+PALP) reconstruction (1730–2013 CE) based on raw data, periods of negative anomalies were shown in the 1740s–1760s, 1800s–1840s, 1880s, and 1960s–1970s (Fig. 5). However, the PC1 (ANBO+PALP) reconstruction (1611–2015 CE) reported negative anomalies in the 1620s–1630s and 1690s and, coherently with the previous 1750s, 1800s–1830s, 1880s, and 1960s–1970s (Fig. 5). The reconstruction performed considering only the ANBO chronology (1502–2015 CE) revealed negative anomalies in the 1500s–1520s, 1580s–1600s, 1620s–1670s, and as well as in other proposed reconstructions in the 1690s–1710s, 1750s, 1790s–1850s, 1870s–1910s, and 1960s–1970s (Fig. 5). These cool periods were alternated by periods with positive anomalies that exceeded the symbolic threshold of +1 °C over the 1961–1990 mean, starting from the 2000s. More specifically, there were particular years in which the anomaly value exceeded two standard deviations from the reconstruction anomaly mean (Table 3). Evidently, after the 1850s, the number of years with particularly negative anomalies rapidly decreased, whereas the number of years with exceptionally positive anomalies increased.

| Cal. period | $R^2_{cal}$* | DW | CCV* | BTFS† |
|---|---|---|---|---|

| Predictor | Negative anomaly year [CE] | | | RE | Positive anomaly year [CE]CE | Intercept-ratio | Slope-ratio | $R^2$-ratio |
|---|---|---|---|---|---|---|---|---|
| Raw | PC1 (ANBO+BARC+PALP) [17301800–1906 1907–2013 CE] | 1753 1754 1813 1814 1815 1816 1819 1821 1830 1838 1880 1889 1956 19640.51±0.07 0.45±0.08 | 2003 20091.71 1.22 | 0.51±0.01 0.44±0.01 | – 0.17±0.10 – 0.20±0.15 | [0.886÷0.931] | [0.617÷1.153] | [0.750÷1.859] |
| PC1 (ANBO+PALP) [1611 2015 CE]Low | 1628 1633 1675 1753 1754 1813 1814 1815 1816 1819 1821 1830 1841 1880 1884 1909 1956 19641800–1906 1907–2013 | 2003 2005 2007 2009 20120.72±0.05 0.51±0.06 | 0.04 0.01 | 0.71±0.00 0.50±0.01 | – 1.08±0.11 – 2.43±0.52 | [0.893÷0.919] | [0.579÷0.879] | [1.106÷1.875] |
| ANBO [1502 –2015 CE]High | 1515 1524 1628 1633 1675 | 1548 1994 2003 2005 2007 2009 2012 20131800–1906 1907–2013 | 0.37±0.08 0.25±0.07 | 2.19 2.23 | 0.35±0.01 0.23±0.02 | 0.23±0.01 0.34±0.02 | [–13.272÷10.634] | [0.683÷1.587] | [0.749÷2.529] |

Celle inserite
Celle inserite
Celle inserite
Celle inserite
Celle inserite
Celle inserite
Celle inserite
Celle inserite
Celle inserite
Celle eliminate
Celle inserite

5
169
9
172
1
175
3
175
4
181
3
181
4
181
5
181
6
181
9
182
1
183
0
184
1
188
8
190
9
195
6

Table 3: particularly

According to the PC1 (ANBO+BARC+PALP) JJA reconstruction (1730–2013 CE) based on raw data, periods of negative temperature anomalies, considering 1901–2000 as the reference period, were obtained in the 1740s–1850s, 1880s–1910s, and

1960s–1980s (Fig. 5). The PC1 (ANBO+PALP) reconstruction (extending back to 1611 CE, lengthening the previous by 119 years) reported negative anomalies in the 1610s–1640s, 1660s, and 1690s–1710s, in addition to those reported by PC1 (ANBO+BARC+PALP; Fig. 5). The reconstruction performed considering only the ANBO DBI site chronology (extending back to 1502 CE, lengthening the reconstruction based on PC1 (ANBO+BARC+PALP) by 228 years) revealed negative anomalies in the 1500s–1520s and 1570s–1670s, in addition to those reported in other proposed reconstructions (Fig. 5). These cool periods were intercalated by periods with positive anomalies. Starting in the 2000s, the reconstructed temperature anomalies exceeded the symbolic threshold of +1 °C over the 1901–2000 mean. Interestingly, after the 1850s, the number of years with particularly negative anomalies (i.e., anomalies whose values deviate by at least two standard deviations from the reconstruction 1901–2000 anomaly mean) rapidly decreased, whereas the number of years with exceptionally positive anomalies increased (Table 3).

**Table 3: Particularly cold or warm years in which anomaly values differ by at least two standard deviations from the mean. of the reference period (1901–2000).**

| Predictor | Negative anomaly year [CE] | Positive anomaly year [CE] |
|---|---|---|
| PC1 (ANBO+BARC+PALP) [1730–2013 CE] | 1743 1753–1756 1810 1813–1817 1819 1821 1835 1838 1841 1880 1884 1889 1909 1975 1978 | 1994 2003 2005 2007 2009 2012 |
| PC1 (ANBO+PALP) [1611–2015 CE] | 1628 1632 1633 1675 1690 1754 1755 1810 1813–1817 1819 1821 1841 1884 1889 1909 1975 1978 | 1994 2003 2005 2007 2009 2012 |
| ANBO [1502–2015 CE] | 1512–1514 1516 1628 1631–1633 1639 1675 1698–1700 1754 1810 1813–1817 1819 1821 1825 1830 1835 1838 1841 1884 1888 1891 1909 | 1764 1994 1998 2003 2005 2007 2009 2012 2013 |

## 5 Discussion

The data presented here represent are, to our knowledge, the first attempt to use European larch BI data for dendroclimatic purposes in the European Alps.. In fact, currently, only one other study has used BI data from for this species but for dendroentomological purposes (Arbellay et al., 2018), whereas; moreover, considering other alpine species, only a few studies with dendroclimatic purposes exist for have explored the BI–climate relationships in this area but focused on other alpine species (Cerrato et al., 2023; Frank and Nicolussi, 2020; Österreicher et al., 2014; Trachsel et al., 2012; Babst et al., 2009). Consequently, this is also the first approach to dendroclimatic reconstruction based only on the BI of larches in the Southern Rhaetian Alps but also for the European Alps in general.

Regarding the different percentages of lighter (or darker) pixels, a total of 24 chronologies were obtained for their analysis. Preliminary analyses allowed us to observe slight differences in correlation values between the BI and climate data as a function

of the considered pixel percentage (for both the EWBI and LWBI). The highest correlation was obtained for the DBI chronology derived from the difference between the mean of the pixels belonging to the first darker quartile (25 % of the LWBI pixels) and the mean of the pixels belonging to the whole earlywood (100 % of the EWBI pixels; not shown); thus, this chronology was used for successive analysis and considerations. Since the aim of this study was to verify the possibility of using BI data from European larch as a climate proxy, a detailed study on the mechanism that drove differences in correlation and thus the amount of explained variance as a predictor is worthy of future investigation but beyond the scope of this study. However, the highlighted slight influence of the considered percentage of pixels on the correlation with climate is corroborated by a previous study performed using Swiss stone pine (*Pinus cembra* L.), which attributed greater importance to the sampling polishing process than to the considered pixel amount or extractives removal process (Cerrato et al., 2023).

The considered DBI site chronologies showed highly coherent behaviour, confirmed by the high correlation values (Table 1), by both the high explained variance of the first principal component (82.32 %) and by the stability of the EPCA analysis (Fig. S2 in the Supplementary Material). Moreover, since the samples in this study were not washed in a Soxleth apparatus, it is important to highlight that no evident offset between sapwood and heartwood sample data was noticeable in the DBI chronologies of all the sites (Fig. 2). This led to the speculation that, unlike for other species (e.g.,. This gap in knowledge implies that no standard procedures exist for researching samples. In this study, according to Wilson et al. (2021, 2019, 2014) and others (Heeter et al., 2020; Arbellay et al., 2018; Dolgova, 2016; Dannenberg and Wise, 2016), the samples were not treated with solvent for resin and extractive removal. It is known that in resinous species, the presence of resins and other extractives could hamper BI measurements (Wilson et al., 2021; Rydval et al., 2014); on the other hand, on some species, the creation of DBI chronologies successfully corrects the issues due to the discolouration that occurs at heartwood-sapwood transition and in resinous zones of the samples (Reid and Wilson, 2020; Fuentes et al., 2018; Wilson et al., 2017a; Björklund et al., 2015, 2014). The larch DBI chronologies obtained in this study did not exhibit sharp differences in values between sapwood and heartwood (Fig. 2) compared with the EWBI and LWBI chronologies (Fig. S3 in the Supplementary Material). This led to the conclusion that unlike for other species (e.g., *Pinus sylvestris* and *Manoao colensoi*; Seftigen et al., 2020; Blake et al., 2020; Fuentes et al., 2018), the simple DBI chronology could be sufficient for obtaining a good and reliable climate proxy for European larch, at least for samples collected from living individuals. This does not exclude the possibility that the removal of extractives, the adjustment of the BI values (Björklund et al., 2015), and/or the use of regional curve standardization (Helama et al., 2017) together (or not) with a signal-free approach (McPartland et al., 2020; Melvin and Briffa, 2008) will improve the already high regression performances.creation of a DBI chronology in the European larch could be suitable for correcting discolouration bias due to heartwood-sapwood transition, at least for samples collected from living individuals not affected by fungal or bacterial activity or decay. This hypothesis is also corroborated by the moving correlation analysis, which shows a rapid decrease in correlation values at the most recent end when considering the EWBI PC1 (ANBO+BARC+PALP) and LWBI PC1 (ANBO+BARC+PALP) chronologies (Fig. S5 in the Supplementary Material). In contrast, DBI PC1 (ANBO+BARC+PALP) showed an upwards trend in correlation values (Fig. 3). Our results strengthen the hypothesis that if the EWBI and LWBI are influenced by diachronic or different climate parameters (e.g., precipitation and/or temperature), the

use of the DBI emphasizes climate signals (Blake et al., 2020). In fact, considering the high-frequency domain, the EWBI PC1 (ANBO+BARC+PALP) results are affected by the current July and April mean temperatures, whereas the LWBI is influenced by the current June–August and JJA mean temperatures (Fig. S5 in the Supplementary Material).

### 5.1 BI–climate correlation

~~Static~~The correlation analyses highlighted the strong influence of the summer (i.e., June~~–~~ to August) monthly mean temperature on the PC1 ~~DBI~~(ANBO+BARC+PALP) chronology (Fig. 3a). ~~Similar but lower results were also obtained for the mean minimum and maximum temperatures.~~ These high correlation values with ~~June–August~~monthly mean temperatures and even greater ~~correlation~~correlations with JJA mean temperatures indicate that the ~~common~~ signal observable in the ~~chronologies~~chronology is due to the influence of this specific climatic parameter on tree growth. These observations ~~underline~~indicate that BI responds to the same limiting factors that ~~also~~ affect other well-studied tree-ring parameters (e.g., maximum wood density and total ring width~~)~~), both in the area (Cerrato et al., 2018; Coppola et al., 2013) and in the Alps (Leonelli et al., 2016; Büntgen et al., 2011, 2006, 2005; Frank and Esper, 2005), even if spatial and/or physiological heterogeneity in the climate response within the species may exist (Saulnier et al., 2019; Carrer and Urbinati, 2004). PC1 (ANBO+BARC+PALP) can explain up to 38.4 % (26.7–48.5 %) of the JJA mean temperature variance in the study area; this result is 70 % greater than the percentage of temperature variance explained by TRW in the area (Cerrato et al., 2018) and, depending on the reference period, comparable to the results obtained by using MXD data (Büntgen et al., 2006). This finding reinforces the idea that DBI could also be considered a better predictor than the ring width for summer temperatures for the European larch.

The moving correlation function between PC1 (ANBO+BARC+PALP) and the mean temperature (Fig. 3b) shows a relatively stable correlation in the raw data and in the high-frequency domain. Previous TRW-based studies in the same area (Cerrato et al., 2018; Coppola et al., 2013, 2012) have indicated a reduction in the correlation between tree-ring parameters and climate since the 1960s; this correlation reduction is known as the "divergence problem" (Anchukaitis et al., 2017; Wilson et al., 2016; D'Arrigo et al., 2008; Büntgen et al., 2008, 2006). Our results showed that, compared with the use of TRW chronologies, the use of BI data mitigated the influence of divergence (Cerrato et al., 2018; Coppola et al., 2012), as similarly reported for Swiss stone pine in the same area (Cerrato et al., 2023), for Norway spruce (*Picea abies* (L.) H. Karst.) in the Carpathians (Buras et al., 2018) and for white spruce (*Picea glauca* (Moench) Voss) in ~~The moving correlation function between the PC1 DBI and mean temperature (Fig. 3b) highlights a relatively stable correlation in the raw data and high-frequency domain, with an impactful decrease in the correlation coefficients in 1964 CE and 2003 CE. The decrease recorded since 1964 CE is imputable to a known outlier in the BI data (Fig. 3c). In fact, the 1964 CE was characterized by one of the worst larch budmoth (*Zeiraphera diniana* Gn.) outbreaks in the area (Baltensweiler and Rubli, 1999), as reported in a previous total-ring-width analysis (Cerrato et al., 2019b; Turchin et al., 2003). Moreover, considering the occurrence of larch budmoth outbreaks in the area, most of the other particularly negative anomalies can be tentatively associated with parasite outbreaks (e.g., 1956, 1909, 1888/89, 1884, 1880, 1841, 1838, 1830, 1821, 1753/54, 1721 CE; Table 3; Cerrato et al., 2019b; Arbellay et al., 2018; Büntgen~~

et al., 2009). Conversely, the 2003 CE was influenced by the meteoclimatic conditions that occurred during that summer (Beniston, 2004; Fink et al., 2004). Despite the coherence shown by the DBI data and temperature time series in this year, denoting the relatively good performance of the DBI data for identifying even meteorological extremes, a sudden increase in the correlation coefficient (Fig. 3b) could be considered a methodological artefact due to the effect of these outliers on the correlation values (Fig. S5 in the Supplementary Material). In fact, if the 1964 CE is removed, the sudden decrease is also removed, and the moving correlation values assume more linear behaviour (Fig. the Yukon in North America (Wilson et al., 2019). In fact, in recent decades, contrary to the correlation values obtained between TRW and mean temperatures, the correlation values between BI data and mean temperature increased, highlighting the reduced effect of the 'divergence problem' on the raw data and in the high-frequency domain (Fig. 3b).

S5 in the Supplementary Material). Nevertheless, although the raw data correlation values do not show any monotonic trend, the correlation values between the DBI and JJA temperature, considering the whole correlation series in the high-frequency domain, preserve their negative trend even if known outliers (i.e., 1964 and 2003 CE) are removed, but show a significant upward trend if the trend analysis is focussed on 1960–2013 period (Mann-Kendall S: 379; p-value<0.01).

Previous analysis performed on TRW in the same study area (Cerrato et al., 2018; Coppola et al., 2013, 2012) reported the reduction in the correlation between tree-ring parameters and climate in the most recent portion of the chronologies. This is an issue known as the 'divergence problem' (D'Arrigo et al., 2008). The divergence problem is ubiquitous but aleatory in the Northern Hemisphere (Anchukaitis et al., 2017; Wilson et al., 2016; Büntgen et al., 2008), and it was observed especially when total ring width was considered, whereas it was attenuated when other tree-ring parameters were used (Büntgen et al., 2006). Among the other, standardization method could be one sources of the divergence (D'Arrigo et al., 2008), however, applying best practice of detrending, this issue could be attenuated (Ols et al., 2023). In the study area, the results showed that the use of BI data attenuated the influence of divergence compared to the use of TRW chronologies (Cerrato et al., 2018; Coppola et al., 2012), as similarly reported for Swiss stone pines in the same area (Cerrato et al., 2023), for Norway spruce (*Picea abies* (L.) H. Karst.) in the Carpathian Mountains (Buras et al., 2018) and for white spruce (*Picea glauca* (Moench) Voss) in Yukon, North America (Wilson et al., 2019). However, due to the continuity of the decrease highlighted by the high-frequency domain along the entire correlation series (even if a significant upward trend with values around $r = 0.50$ is appreciable in the last decades, especially if 1964 and 2003 CE outliers were removed; Fig. 3b and Fig. S5 in the Supplementary Material) and considering that, in most cases, the 'divergence problem' in the area started to affect the correlation with TRW in the 1960s (Cerrato et al., 2018; Coppola et al., 2012), other factors apart standardization should be considered causes of the loss of explanatory power along the series, and probably not ascribable to the 'divergence problem' *sensu stricto*. Initially, we speculate that since a decrease in correlation affects the high-frequency domain and thus the quasiannual variation, the standardization method used should not have a relevant role. On the other hand, changes in climatic conditions, such as a more important role of precipitation quantity and distribution related to higher temperatures and thus an enhanced drought signal embedded in the series, could be an alternative explanation for the observed correlation pattern. However, additional studies are needed to better understand the observed trends in correlation values. On the other hand, considering correlations

~~coefficients, in the last decades, contrarily to the correlation values obtained between TRW and mean temperatures, the values increased, denoting the absence of the 'divergence problem' in the raw series and the influence of the low frequencies on correlation values.~~

Spatial correlations highlight that the BI data are representative not only of the local temperature but also, as expected, of the spatial homogeneity of this climatic parameter (Brunetti et al., 2006), which is also representative of a broader area (Fig. 4). ~~Specifically, the raw data reveal high and significant values across an area spanning from the Mediterranean basin to the Middle East, North Africa and the Arabian Peninsula (Fig. 4a). However, this significant correlation and its wide spatial representativeness are not stable over time. In fact, starting from positive significant values calculated only over the Mediterranean basin at the beginning of the time series, these values widely and rapidly expand towards the southeast, broadening the correlation significance in the last portion of the time series (Fig. S3, Animation S1 in the Supplementary Material). This enlargement is consistent with what is observed at the local site (Fig. 3b), where the raw data show a rapid increase in correlation values, probably due to the retention of the low frequencies in the raw data. In fact, as highlighted by the moving correlation analysis, the low-frequency domain reaches its maximum correlation with the JJA temperature in the last portion of the analysed period, influencing the correlation of the raw data. This hypothesis is also corroborated by the results of the CCV, BTFS and Durbin-Watson tests, which~~The temporal variability of the spatial correlation values reflects the same variability observed with the moving correlation analysis at the local scale both in the raw data and in the high-frequency domain. In fact, the spatial correlation values obtained from the analysis of the raw data show greater variation than those obtained from the analysis in the high-frequency domain. This finding is also consistent with the results of the CCV, BTFS and Durbin-Watson tests performed at the local scale; these results revealed the nonstationarity of the regression intercept between the calibration and verification periods~~, which was even more pronounced in the low-frequency domain (Table 2). The high-frequency domain i) supports the hypothesis of the not-negligible influence of the low-frequency domain in the raw data, and ii) confirms the BI data as a potential proxy with an explanatory power higher than that reported by TRW for the same area (Cerrato et al., 2018; Coppola et al., 2013) and sometimes comparable to those obtained by MXD data (Büntgen et al., 2006), at least at high frequencies, as reported for other alpine species (Cerrato et al., 2023). Its spatial correlation is consistent with previous results, revealing a contraction of the spatial representativeness of the high-frequency band across the whole time series (Fig. S4, Animation S2 in the Supplementary Material), revealing the constant and significant negative trend shown by moving correlation analysis (Fig. 4b), even if stabilized in the last decades.~~ and thus a not completely neglectable influence of the low-frequency domain on the raw data. In fact, the influence of the low-frequency domain on the raw data is not only inferred locally but also spatially represented by a rapid spatial increase in the significant correlation values in the most recent decades (Fig. S8 and Fig. S9 in the Supplementary Material). In contrast, the spatiotemporal variability of correlation values in the high-frequency domain is more limited; this variability is consistent with results obtained at the local scale, thus indicating the stability of the transfer function and thus the reliability of the BI data in the high-frequency domain, as also demonstrated for other species in both the Northern and Southern Hemispheres (Wilson et al., 2021).

### 5.2 Mean June–August temperature reconstruction

The PC1s and the ANBO chronologies showed good predictive ability (Table 3; ~~Tables S1~~Table S2 and ~~S2~~Table S3 in the Supplementary Material), especially in the high-frequency domain. All the tested chronologies had positive RE values, whereas the CE values ~~are~~were positive in the high-frequency domain and slightly negative considering the raw PC1 (ANBO+BARC+PALP) and PC1 (ANBO+PALP) data. These results ~~highlights~~highlight the potential of DBI chronologies as proxies for the selected target climatic factor under certain ~~condition~~conditions. These ~~results~~findings are corroborated by ~~the~~ more rigorous BTFS tests (Buras et al., 2017), where the ~~PC1~~PC1's raw chronologies exhibit instability in terms of the regression offset parameter (Table 3 and Table ~~S1~~S2 in the Supplementary Material), implying weak nonstationarity in the trend (described by scenario I in Buras et al., 2017~~), whereas the ANBO-based reconstruction reveals nonstationarity in the regression slope and, as a consequence, in the explained variance, which is the cause of major trend instability (outlining scenarios II and III in Buras et al., 2017), and implies nonstationarity of the transfer function in the low-frequency domain.~~). The nonstationarity of tree-ring proxies is widespread, and its presence in BI data has already been assessed in other species (e.g., Engelmann spruce, *Picea engelmannii* Parry ex Engelm. (Wilson et al., 2014)~~,~~; Scot pine, *Pinus sylvestris* L. (Rydval et al., 2016)~~,~~; and Swiss stone pine (Cerrato et al., 2023)), reflecting complex biological environmental-growth interactions (Wilmking et al., 2020) as well as complex interactions among abiotic entities (i.e., glaciers), biological growth and the environment (Cerrato et al., 2020; Leonelli et al., 2011). Analysis in the high-frequency domain, however, always passes the BTFS tests but at the expense of the retained low-frequency ~~trend~~, which is relevant for climatic reconstructions (Esper et al., 2002)~~,~~ and must be reintegrated to obtain reliable long-term reconstructions (Rydval et al., 2016).

Based on these assumptions, raw data-based reconstructions ~~have been~~were performed considering PC1s and ANBO chronologies, supposing that ~~a~~the weak nonstationarity of the transfer function returned more useful information than ~~those obtainable~~that obtained by the deletion of the entire low-frequency band, at least at this preliminary stage of the study. A comparison between the reconstructed JJA temperature and both instrumental data (Fig. 5a) and previously proposed reconstructions (Fig. 5b–d) reveals good agreement between the considered series. Generally, the DBI-based JJA temperature reconstruction proposed here returns completely comparable anomalies. The slight overestimation of the anomalies is noticeable when the comparison with instrumental data or ~~total ring width and~~ maximum wood density-based reconstruction are considered (Fig. 5a and Fig. 5d), as exclusion of the more recent period, where an underestimation occurs. Nevertheless, local tree-ring based and multiproxy ~~data~~based reconstructions (Fig. ~~5a~~5b ~~–~~c) corroborate the validity of the proposed BI-based reconstruction, agreeing well with respect to the trend and within the calculated RMSE. ~~The~~In fact, the highest concordance was observed with local data obtained by total ring width reconstruction (Coppola et al., 2013), ~~which used~~based on chronologies from ~~other~~adjacent valleys ~~of one of the massifs~~ to those sampled ~~here (i.e., Adamello–Presanella),~~for this study, and from multiproxy-based reconstruction (Trachsel et al., 2012). ~~Comparing the performance of the regression against the temperature of both the DBI and TRW data of ANBO, the only here used site chronology for which a TRW-based temperature reconstruction exists (Cerrato et al., 2018), the regression involving DBI data returned higher indices and thus results better~~

~~correlated (with higher predictive ability) with JJA temperatures than the latewood width with June–July mean temperatures (the meteorological variable that return the higher regression parameters considering the ring width). This reinforce the idea that DBI could be considered a better predictor than ring widths for summer temperatures also for European larch.~~

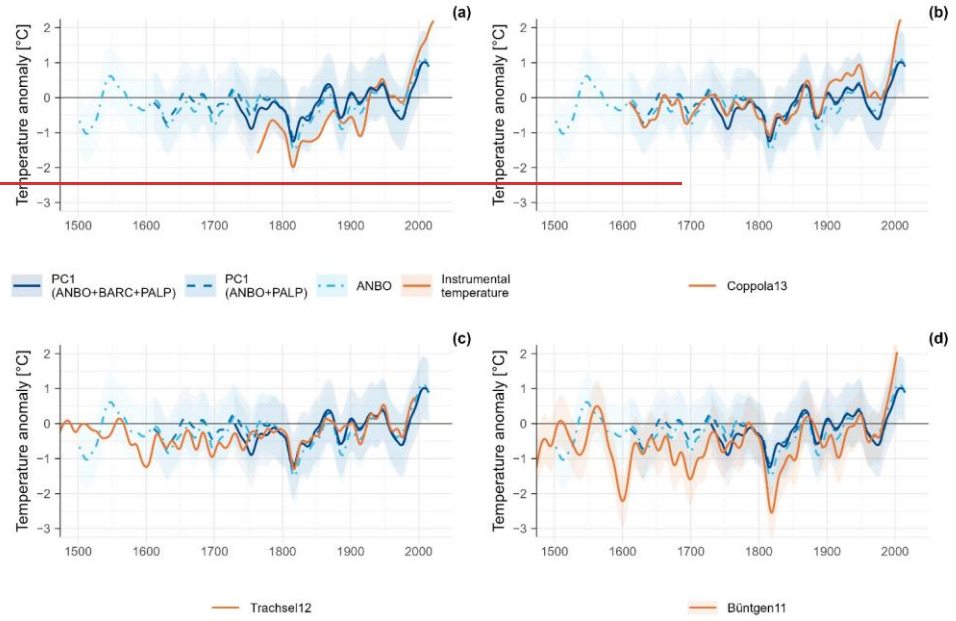

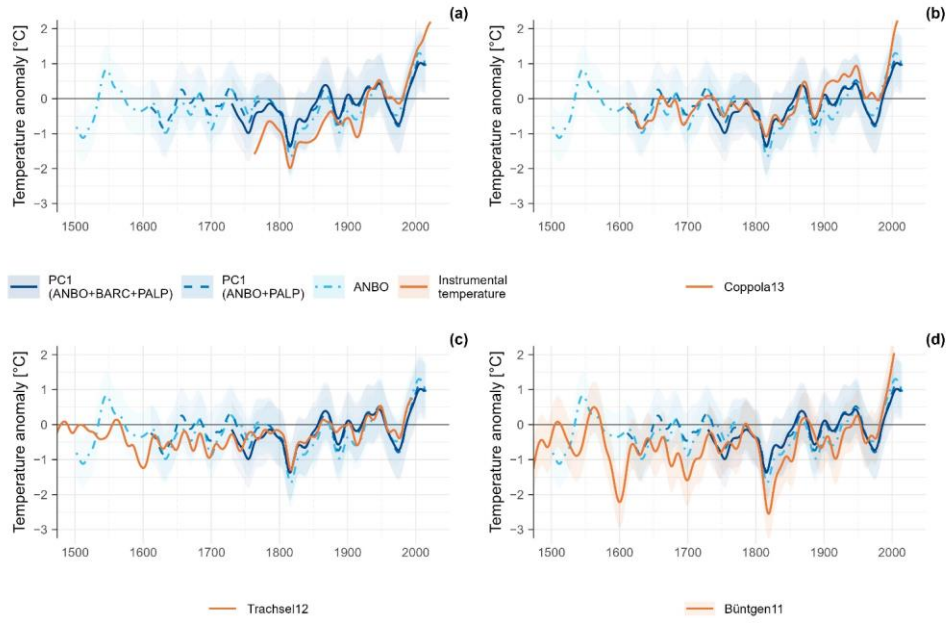


**Figure 5: Comparison between DBI PC1 and meteorological data (a) or the previously published JJA reconstruction (b–d). The solid, dashed and dotted blue lines are the JJA reconstructions performed considering the DBI PC1 of ANBO, BARC and PALP (1730–2013), ANBO and PALP (1611–2015), or only the ANBO chronology (1502–2015), respectively. The shaded area identifies the lower and upper confidence intervals at 95 %, where available. (For interpretation of the references to colour in this figure legend, the reader is referred to the web version of this article.)**

When ~~analysing~~we analysed the PC1s-based reconstructed ~~trends~~decadal variabilities, these ~~are~~variations were corroborated by well-known climatic dynamics in the Alps. In fact, the cold phases reconstructed between the 17$^{th}$ and 19$^{th}$ centuries agree well with the known local acmes of the Little Ice Age (LIA), a period ~~generally characterized by low temperature.~~well known for colder climatic conditions. During the LIA, the glaciers in the area, as well as along the entire alpine range, ~~reach~~reached their Holocene maximum extension, even if ~~asynchronously~~diachronically within the 17$^{th}$–mid-19$^{th}$ centuries (Cerrato et al., 2020; Zemp et al., 2015; Carturan et al., 2014, 2013). Regarding the oldest portion of the ANBO raw-based reconstruction, ~~even considering the major trend non-stationarity highlighted by the BTFS tests (Table S2 in the Supplementary Material), the behaviour~~the variability of the anomalies is very similar to ~~the trend~~that reported by total ring width-based reconstruction (Cerrato et al., 2018), and ~~it~~ is probably influenced by anthropogenic activities and wood harvesting and/or management performed in the area in the 16$^{th}$ century (Backmeroff, 2001). Moreover, despite the gap-filling procedure applied to the BI

core series (Büntgen et al., 2006), some of the particularly negative anomalies observed are coeval to LBM outbreaks reported in the surrounding area (i.e., 1753/54, 1821, 1830, 1838, 1841, 1880, 1884, 1888/89, and 1909 CE; Table 3; Cerrato et al., 2019b; Arbellay et al., 2018; Büntgen et al., 2009).

After the coolest phases of the LIA, a progressive noncontinuous increase in the reconstructed JJA anomalies is evident and is corroborated by other reconstructions and instrumental data (Fig. 5). In fact, JJA temperature anomalies started ~~and continue~~ to ~~grow between~~increase in the 1850s ~~and today~~, with a major hiatus occurring during the 1970s–1980s. This latter cooling phase is corroborated by instrumental data, other reconstructions, and environmental evidence that reported the last readvance of some glaciers in the area during this period (Salvatore et al., 2015). After the 1980s, the highest anomaly values of the entire series were reported, in accordance with more recent climate dynamic evidence (IPCC, 2018). Indeed, during this last phase, ~~the majority~~most of the positive anomalies are identified (Table 3), and they almost correspond with years that are known for their exceptionally warm ~~temperature~~temperatures across the European Alps (IPCC, 2018; Beniston, 2004; Fink et al., 2004).

## 6 Conclusions

~~In this paper, we focus on the utilization of European larch within the Southern Rhaetian Alps, demonstrating its potential for providing insights into the region's climate history. Specifically, we explored the application of blue intensity (BI), a relatively novel technique, to obtain a proxy with predictive skills similar to those shown by using MXD data. In this context, the application of BI data analysis offers a promising tool for enhancing our understanding of past climate dynamics in the study area and regionally by providing additional information to those retrieved from other methodologies (e.g., TRW, MXD, wood anatomical traits and isotopes). In fact, the obtained results show that the BI data are representative of the mean JJA temperature at both the local and regional scales. The obtained data and their predictive ability are supported by the positive results obtained by more rigorous tests of regression stationarity, highlighting the positive predictive ability of BI for European larch, as well as for other coniferous species already tested in the area and worldwide, at least in high-frequency domain. Some issues regarding the long-term trend persist and are worthy of future investigation. Moreover, opening the possibility of integrating the use of BI data with more traditional dendrochronological techniques widely applied to European larch in the Alps, this study represents not only a first step towards promoting the use of BI data as a surrogate of MXD data in the European Alps but also the possibility of obtaining MXD-like data from a greater number of laboratories for a highly investigated species to address critical questions related to the historical climate of the Southern Rhaetian Alps and the Alps in general.~~

**~~Author contribution~~**

In this paper, we focus on the employment of the European larch within the Southern Rhaetian Alps, thus demonstrating its potential for providing insights into the region's climate history. Specifically, we explored the application of blue intensity

(BI), a relatively novel technique, to obtain a proxy with predictive skills like those shown by using MXD data. In this context, the application of BI data analysis offers a promising tool for enhancing our understanding of past climate dynamics in the study area and regionally by providing information additional to that retrieved from other methodologies (e.g., TRW, MXD, wood anatomical traits and isotopes). In fact, the obtained results show that the BI data are representative of the mean JJA temperature at both the local and regional scales. The obtained data and their predictive ability are supported by the positive results obtained by more rigorous tests of regression stationarity, thus highlighting the positive predictive ability of BI for the European larch and for other coniferous species already tested in the area and worldwide, at least in the high-frequency domain. Although the results obtained from using BI from the European larch to reconstruct temperature changes are very encouraging, methodological studies are certainly worthy of further investigation. Particular attention must be given to the effects of i) removing extractives, ii) adjusting BI values (Björklund et al., 2015), iii) scanning resolution and BI frame size, and iv) regional curve standardization (Helama et al., 2017) combined (or not) with a signal-free approach (McPartland et al., 2020; Melvin and Briffa, 2008). On the other hand, opening the possibility of integrating the use of BI data with more traditional dendrochronological techniques applied to the European larch in the Alps, the methods we employed represent not only a first step towards promoting the use of BI data as a surrogate of MXD in the European Alps but also the possibility of obtaining MXD-like data from more laboratories to address critical questions related to historical climate variations in the Alpine region.

## Author contributions

**Riccardo Cerrato**: Conceptualization (equal); ~~Data~~data curation (equal); ~~Formal Analysis; Investigation~~formal analysis; investigation (lead); ~~Methodology~~methodology (lead); ~~Project~~project administration; ~~Visualization; Writing~~visualization; writing – original draft. **Maria Cristina Salvatore**: Conceptualization (equal); ~~Data~~data curation (equal); ~~Supervision~~supervision (equal); ~~Writing~~writing – review ~~&~~and editing (equal). **Michele Brunetti**: Data curation (equal); ~~Methodology~~methodology (supporting); ~~Writing~~writing – review ~~&~~and editing (equal). **Andrea Somma**: Investigation (supporting). **Carlo Baroni**: Conceptualization (equal); ~~Funding~~funding acquisition; ~~Resources; Supervision~~resources; supervision (equal); ~~Writing~~writing – review ~~&~~and editing (equal).

## Competing interests

Any use of trade, firm, or product names is for descriptive purposes only and does not imply endorsement by the in- volved universities. The authors declare that they have no ~~conflict~~conflicts of interest or competing interests.

**Acknowledgements**

This research was supported by the Laboratory of ~~dendrochronology~~Dendrochronology of the Department of Earth Sciences (University of Pisa). We are very grateful to Dr. Gino Delpero and Luca Colato, Custodi Forestali of Comune di Vermiglio, and to the staff of the Stazione Forestale of the Comune di Ossana (TN) for helping in field activities and sampling. We wish to thank Dr. Fabio Angeli, responsible for the Ufficio Distrettuale Forestale di Malè (TN), for sampling permission. The Scientific colour maps are used in this study to prevent visual distortion of the data and exclusion of readers with colour-vision deficiencies.

**References**

Anchukaitis, K. J., Wilson, R., Briffa, K. R., Büntgen, U., Cook, E. R., D'Arrigo, R. D., Davi, N., Esper, J., Frank, D. C., Gunnarson, B. E., Hegerl, G., Helama, S., Klesse, S., Krusic, P. J., Linderholm, H. W., Myglan, V. S., Osborn, T. J., Zhang, P., Rydval, M., Schneider, L., Schurer, A., Wiles, G. C., and Zorita, E.: Last millennium Northern Hemisphere summer temperatures from tree rings: Part II, spatially resolved reconstructions, Quat. Sci. Rev., 163, 1–22, https://doi.org/10.1016/j.quascirev.2017.02.020, 2017.

Andreis, C., Armiraglio, S., Caccianiga, M., Bortolas, D., and Broglia, A.: Pinus Cembra L. nel settore sud-Alpino Lombardo (Italia Settentrionale), Nat. Brescia. - Ann. Mus. Civ. Sc. Nat., Brescia, 34, 19–39, 2005.

Arbellay, E., Jarvis, I., Chavardès, R. D., Daniels, L. D., and Stoffel, M.: Tree-ring proxies of larch bud moth defoliation: Latewood width and blue intensity are more precise than tree-ring width, Tree Physiol., 38, 1237–1245, https://doi.org/10.1093/treephys/tpy057, 2018.

Auer, I., Böhm, R., Jurkovic, A., Lipa, W., Orlik, A., Potzmann, R., Schöner, W., Ungersböck, M., Matulla, C., Briffa, K. R., Jones, P., Efthymiadis, D., Brunetti, M., Nanni, T., Maugeri, M., Mercalli, L., Mestre, O., Moisselin, J.-M., Begert, M., Müller-Westermeier, G., Kveton, V., Bochnicek, O., Šťastný, P., Lapin, M., Szalai, S., Szentimrey, T., Cegnar, T., Dolinar, M., Gajic-Capka, M., Zaninović, K., Majstorović, Ž., and Nieplova, E.: HISTALP—historical instrumental climatological surface time series of the Greater Alpine Region, Int. J. Climatol., 27, 17–46, https://doi.org/10.1002/joc.1377, 2007.

Babst, F., Frank, D. C., Büntgen, U., Nievergelt, D., and Esper, J.: Effect of sample preparation and scanning resolution on the Blue Reflectance of Picea abies, TRACE–Tree Rings Archaeol. Climatol. Ecol., 7, 188–195, 2009.

Backmeroff, C. E.: Historical land-use and upper timberline dynamics determined by a thousand-year larch chronology made up of charcoal fragments from kilns and ancient trees, in: International Conference Tree Rings and People, 1–2, 2001.

Baltensweiler, W. and Rubli, D.: Dispersal: an important driving force of the cyclic population dynamics of the larch bud moth, Zeiraphera diniana Gn., For. Snow Landsc. Res., 74, 3–153, 1999.

Beniston, M.: The 2003 heat wave in Europe: A shape of things to come? An analysis based on Swiss climatological data and model simulations, Geophys. Res. Lett., 31, https://doi.org/10.1029/2003GL018857, 2004.

Biondi, F. and Waikul, K.: DENDROCLIM2002: A C++ program for statistical calibration of climate signals in tree-ring

chronologies, Comput. Geosci., 30, 303–311, https://doi.org/10.1016/j.cageo.2003.11.004, 2004.

Björklund, J., Gunnarson, B. E., Seftigen, K., Esper, J., and Linderholm, H. W.: Blue intensity and density from northern Fennoscandian tree rings, exploring the potential to improve summer temperature reconstructions with earlywood information, Clim. Past, 10, 877–885, https://doi.org/10.5194/cp-10-877-2014, 2014.

Björklund, J., Gunnarson, B. E., Seftigen, K., Zhang, P., and Linderholm, H. W.: Using adjusted Blue Intensity data to attain high-quality summer temperature information: A case study from Central Scandinavia, Holocene, 25, 547–556, https://doi.org/10.1177/0959683614562434, 2015.

Björklund, J., von Arx, G., Nievergelt, D., Wilson, R., Van den Bulcke, J., Günther, B., Loader, N. J., Rydval, M., Fonti, P., Scharnweber, T., Andreu-Hayles, L., Büntgen, U., D'Arrigo, R., Davi, N., De Mil, T., Esper, J., Gärtner, H., Geary, J., Gunnarson, B. E., Hartl, C., Hevia, A., Song, H., Janecka, K., Kaczka, R. J., Kirdyanov, A. V., Kochbeck, M., Liu, Y., Meko, M., Mundo, I., Nicolussi, K., Oelkers, R., Pichler, T., Sánchez-Salguero, R., Schneider, L., Schweingruber, F., Timonen, M., Trouet, V., Van Acker, J., Verstege, A., Villalba, R., Wilmking, M., and Frank, D.: Scientific Merits and Analytical Challenges of Tree-Ring Densitometry, Rev. Geophys., 57, 1224–1264, https://doi.org/10.1029/2019RG000642, 2019.

Björklund, J., Seftigen, K., Fonti, P., Nievergelt, D., and von Arx, G.: Dendroclimatic potential of dendroanatomy in temperature-sensitive Pinus sylvestris, Dendrochronologia, 60, 125673, https://doi.org/10.1016/j.dendro.2020.125673, 2020.

Björklund, J., Fonti, M. V., Fonti, P., Van den Bulcke, J., and von Arx, G.: Cell wall dimensions reign supreme: cell wall composition is irrelevant for the temperature signal of latewood density/blue intensity in Scots pine, Dendrochronologia, 65, 125785, https://doi.org/10.1016/j.dendro.2020.125785, 2021.

Blake, S. A. P., Palmer, J. G., Björklund, J., Harper, J. B., and Turney, C. S. M.: Palaeoclimate potential of New Zealand Manoao colensoi (silver pine) tree rings using Blue-Intensity (BI), Dendrochronologia, 60, 125664, https://doi.org/10.1016/j.dendro.2020.125664, 2020.

Böhm, R., Auer, I., Brunetti, M., Maugeri, M., Nanni, T., and Schöner, W.: Regional temperature variability in the European Alps: 1760-1998 from homogenized instrumental time series, Int. J. Climatol., 21, 1779–1801, https://doi.org/10.1002/joc.689, 2001.

Brunetti, M., Maugeri, M., Monti, F., and Nanni, T.: Temperature and precipitation variability in Italy in the last two centuries from homogenised instrumental time series, Int. J. Climatol., 26, 345–381, https://doi.org/10.1002/joc.1251, 2006.

Brunetti, M., Lentini, G., Maugeri, M., Nanni, T., Auer, I., Böhm, R., and Schöner, W.: Climate variability and change in the Greater Alpine Region over the last two centuries based on multi-variable analysis, Int. J. Climatol., 29, 2197–2225, https://doi.org/10.1002/joc.1857, 2009.

Brunetti, M., Lentini, G., Maugeri, M., Nanni, T., Simolo, C., and Spinoni, J.: Projecting North Eastern Italy temperature and precipitation secular records onto a high-resolution grid, Phys. Chem. Earth, Parts A/B/C, 40–41, 9–22, https://doi.org/10.1016/j.pce.2009.12.005, 2012.

Brunetti, M., Maugeri, M., Nanni, T., Simolo, C., and Spinoni, J.: High-resolution temperature climatology for Italy: interpolation method intercomparison, Int. J. Climatol., 34, 1278–1296, https://doi.org/10.1002/joc.3764, 2014.

Buckley, B. M., Hansen, K. G., Griffin, K. L., Schmiege, S., Oelkers, R., D'Arrigo, R. D., Stahle, D. K., Davi, N., Nguyen, T. Q. T., Le, C. N., Wilson, R., and D'Arrigo, R. D.: Blue intensity from a tropical conifer's annual rings for climate reconstruction: An ecophysiological perspective, Dendrochronologia, 50, 10–22, https://doi.org/10.1016/j.dendro.2018.04.003, 2018.

Bunn, A. G.: A dendrochronology program library in R (dplR), Dendrochronologia, 26, 115–124, https://doi.org/10.1016/j.dendro.2008.01.002, 2008.

Bunn, A. G.: Statistical and visual crossdating in R using the dplR library, Dendrochronologia, 28, 251–258, https://doi.org/10.1016/j.dendro.2009.12.001, 2010.

Büntgen, U., Esper, J., Frank, D. C., Nicolussi, K., and Schmidhalter, M.: A 1052-year tree-ring proxy for Alpine summer temperatures, Clim. Dyn., 25, 141–153, https://doi.org/10.1007/s00382-005-0028-1, 2005.

Büntgen, U., Frank, D. C., Nievergelt, D., and Esper, J.: Summer temperature variations in the European Alps, A.D. 755-2004, J. Clim., 19, 5606–5623, https://doi.org/10.1175/JCLI3917.1, 2006.

Büntgen, U., Frank, D. C., Wilson, R., Carrer, M., Urbinati, C., and Esper, J.: Testing for tree-ring divergence in the European Alps, Glob. Chang. Biol., 14, 2443–2453, https://doi.org/10.1111/j.1365-2486.2008.01640.x, 2008.

Büntgen, U., Frank, D. C., Liebhold, A. M., Johnson, D. M., Carrer, M., Urbinati, C., Grabner, M., Nicolussi, K., Levanič, T., and Esper, J.: Three centuries of insect outbreaks across the European Alps, New Phytol., 182, 929–941, https://doi.org/10.1111/j.1469-8137.2009.02825.x, 2009.

Büntgen, U., Tegel, W., Nicolussi, K., McCormick, M., Frank, D. C., Trouet, V., Kaplan, J. O., Herzig, F., Heussner, K.-U., Wanner, H., Luterbacher, J., and Esper, J.: 2500 Years of European Climate Variability and Human Susceptibility, Science, 331, 578–582, https://doi.org/10.1126/science.1197175, 2011.

Buras, A., Zang, C., and Menzel, A.: Testing the stability of transfer functions, Dendrochronologia, 42, 56–62, https://doi.org/10.1016/j.dendro.2017.01.005, 2017.

Buras, A., Spyt, B., Janecka, K., and Kaczka, R. J.: Divergent growth of Norway spruce on Babia Góra Mountain in the western Carpathians, Dendrochronologia, 50, 33–43, https://doi.org/10.1016/j.dendro.2018.04.005, 2018.

Camiz, S. and Spada, F.: Checking the stability of correlation of chronologies over time: an example on Pinus pinea L. rings widths, Ann. Silvic. Res., 49, https://doi.org/10.12899/asr-2455, 2023.

Camiz, S., Spada, F., Denimal, J. J., and Piraino, S.: Hierarchical factor classification of dendrochronological time-series, Ann. Silvic. Res., 45, 62–75, https://doi.org/10.12899/asr-1968, 2020.

Carrer, M. and Urbinati, C.: Age-dependent tree-ring growth responses to climate in Larix decidua and Pinus cembra, Ecology, 85, 730–740, https://doi.org/10.1890/02-0478, 2004.

Carrer, M., Dibona, R., Prendin, A. L., and Brunetti, M.: Recent waning snowpack in the Alps is unprecedented in the last six centuries, Nat. Clim. Chang., https://doi.org/10.1038/s41558-022-01575-3, 2023.

Carturan, L., Dalla Fontana, G., and Borga, M.: Estimation of winter precipitation in a high-altitude catchment of the Eastern Italian Alps: Validation by means of glacier mass balance observations, Geogr. Fis. e Din. Quat., 35, 37–48,

https://doi.org/10.4461/GFDQ.2012.35.4, 2012.

Carturan, L., Baroni, C., Becker, M., Bellin, A., Cainelli, O., Carton, A., Casarotto, C., Dalla Fontana, G., Godio, A., Martinelli, T., Salvatore, M. C., and Seppi, R.: Decay of a long-term monitored glacier: Careser Glacier (Ortles-Cevedale, European Alps), Cryosph., 7, 1819–1838, https://doi.org/10.5194/tc-7-1819-2013, 2013.

Carturan, L., Baroni, C., Carton, A., Cazorzi, F., Dalla Fontana, G., Delpero, C., Salvatore, M. C., Seppi, R., and Zanoner, T.: Reconstructing fluctuations of La Mare glacier (Eastern Italian Alps) in the late Holocene: new evidence for a Little Ice Age maximum around 1600 AD, Geogr. Ann. Ser. A, Phys. Geogr., 96, 287–306, https://doi.org/10.1111/geoa.12048, 2014.

Cerrato, R., Salvatore, M. C., Brunetti, M., Coppola, A., and Baroni, C.: Dendroclimatic relevance of "Bosco Antico", the most ancient living European larch wood in the Southern Rhaetian Alps (Italy), Geogr. Fis. e Din. Quat., 41, 35–49, https://doi.org/10.4461/GFDQ.2018.41.3, 2018.

Cerrato, R., Salvatore, M. C., Gunnarson, B. E., Linderholm, H. W., Carturan, L., Brunetti, M., De Blasi, F., and Baroni, C.: A Pinus cembra L. tree-ring record for late spring to late summer temperature in the Rhaetian Alps, Italy, Dendrochronologia, 53, 22–31, https://doi.org/10.1016/j.dendro.2018.10.010, 2019a.

Cerrato, R., Cherubini, P., Büntgen, U., Coppola, A., Salvatore, M. C., and Baroni, C.: Tree-ring-based reconstruction of larch budmoth outbreaks in the Central Italian Alps since 1774 CE, iForest - Biogeosciences For., 12, 289–296, https://doi.org/10.3832/ifor2533-012, 2019b.

Cerrato, R., Salvatore, M. C., Gunnarson, B. E., Linderholm, H. W., Carturan, L., Brunetti, M., and Baroni, C.: Pinus cembra L. tree-ring data as a proxy for summer mass-balance variability of the Careser Glacier (Italian Rhaetian Alps), J. Glaciol., 66, 714–726, https://doi.org/10.1017/jog.2020.40, 2020.

Cerrato, R., Salvatore, M. C., Carrer, M., Brunetti, M., and Baroni, C.: Blue intensity of Swiss stone pine as a high-frequency temperature proxy in the Alps, Eur. J. For. Res., 142, 933–948, https://doi.org/10.1007/s10342-023-01566-9, 2023.

Cook, E. R. and Holmes, R. L.: Users Manual for Program ARSTAN, Tucson, Arizona, 81 pp., 1999.

Cook, E. R., Briffa, K. R., and Jones, P. D.: Spatial regression methods in dendroclimatology: A review and comparison of two techniques, Int. J. Climatol., 14, 379–402, https://doi.org/10.1002/joc.3370140404, 1994.

Coppola, A., Leonelli, G., Salvatore, M. C., Pelfini, M., and Baroni, C.: Weakening climatic signal since mid-20th century in European larch tree-ring chronologies at different altitudes from the Adamello-Presanella Massif (Italian Alps), Quat. Res., 77, 344–354, https://doi.org/10.1016/j.yqres.2012.01.004, 2012.

Coppola, A., Leonelli, G., Salvatore, M. C., Pelfini, M., and Baroni, C.: Tree-ring- Based summer mean temperature variations in the Adamello-Presanella Group (Italian Central Alps), 1610-2008 AD, Clim. Past, 9, 211–221, https://doi.org/10.5194/cp-9-211-2013, 2013.

Corona, C., Guiot, J., Edouard, J.-L., Chalié, F., Büntgen, U., Nola, P., and Urbinati, C.: Millennium-long summer temperature variations in the European Alps as reconstructed from tree rings, Clim. Past, 6, 379–400, https://doi.org/10.5194/cp-6-379-2010, 2010.

Crespi, A., Brunetti, M., Lentini, G., and Maugeri, M.: 1961-1990 high-resolution monthly precipitation climatologies for

Italy, Int. J. Climatol., 38, 878–895, https://doi.org/10.1002/joc.5217, 2018.

Crespi, A., Brunetti, M., Ranzi, R., Tomirotti, M., and Maugeri, M.: A multi-century meteo-hydrological analysis for the Adda river basin (Central Alps). Part I: Gridded monthly precipitation (1800–2016) records, Int. J. Climatol., 41, 162–180, https://doi.org/10.1002/joc.6614, 2021.

D'Arrigo, R. D., Wilson, R., Liepert, B., and Cherubini, P.: On the "Divergence Problem" in Northern Forests: A review of the tree-ring evidence and possible causes, Glob. Planet. Change, 60, 289–305, https://doi.org/10.1016/j.gloplacha.2007.03.004, 2008.

Dannenberg, M. P. and Wise, E. K.: Seasonal climate signals from multiple tree ring metrics: A case study of Pinus ponderosa in the upper Columbia River Basin, J. Geophys. Res. Biogeosciences, 121, 1178–1189, https://doi.org/10.1002/2015JG003155, 2016.

Dixon, P. M.: Bootstrap Resampling, in: Encyclopedia of Environmetrics, Wiley, https://doi.org/10.1002/9780470057339.vab028, 2001.

Dolgova, E.: June-September temperature reconstruction in the Northern Caucasus based on blue intensity data, Dendrochronologia, 39, 17–23, https://doi.org/10.1016/j.dendro.2016.03.002, 2016.

Esper, J., Cook, E. R., and Schweingruber, F. H.: Low-Frequency Signals in Long Tree-Ring Chronologies for Reconstructing Past Temperature Variability, Science, 295, 2250–2253, https://doi.org/10.1126/science.1066208, 2002.

Esper, J., George, S. S., Anchukaitis, K., D'Arrigo, R., Ljungqvist, F. C., Luterbacher, J., Schneider, L., Stoffel, M., Wilson, R., and Büntgen, U.: Large-scale, millennial-length temperature reconstructions from tree-rings, Dendrochronologia, 50, 81–90, https://doi.org/10.1016/j.dendro.2018.06.001, 2018.

Eyring, V., Gillett, N. P., Rao, K. M. A., Barimalala, R., Barreiro Parrillo, M., Bellouin, N., Cassou, C., Durack, P. J., Kosaka, Y., McGregor, S., Min, S., Morgenstern, O., and Sun, Y.: Human Influence on the Climate System, in: Climate Change 2021: The Physical Science Basis. Contribution of Working Group I to the Sixth Assessment Report of the Intergovernmental Panel on Climate Change, edited by: Masson-Delmotte, V., Zhai, P., Pirani, A., Connors, S. L., Péan, C., Berger, S., Caud, N., Chen, Y., Goldfarb, L., Gomis, M. I., Huang, M., Leitzell, K., Lonnoy, E., Matthews, J. B. R., Maycock, T. K., Waterfield, T., Yelekçi, O., Yu, R., and Zhou, B., Cambridge University Press, Cambridge, United Kingdom and New York, NY, USA, 423–552, https://doi.org/10.1017/9781009157896.005, 2023.

Fink, A. H., Brücher, T., Krüger, A., Leckebusch, G. C., Pinto, J. G., and Ulbrich, U.: The 2003 European summer heatwaves and drought -synoptic diagnosis and impacts, Weather, 59, 209–216, https://doi.org/10.1256/wea.73.04, 2004.

Frank, D. C. and Esper, J.: Characterization and climate response patterns of a high-elevation, multi-species tree-ring network in the European Alps, Dendrochronologia, 22, 107–121, https://doi.org/10.1016/j.dendro.2005.02.004, 2005.

Frank, T. and Nicolussi, K.: Testing different Earlywood/Latewood delimitations for the establishment of Blue Intensity data: A case study based on Alpine Picea abies samples, Dendrochronologia, 64, 125775, https://doi.org/10.1016/j.dendro.2020.125775, 2020.

Fritts, H. C. (Ed.): Tree Rings and Climate, Elsevier, London, 582 pp., https://doi.org/10.1016/B978-0-12-268450-0.X5001-

0, 1976.

Fuentes, M., Salo, R., Björklund, J., Seftigen, K., Zhang, P., Gunnarson, B. E., Aravena, J. C., and Linderholm, H. W.: A 970-year-long summer temperature reconstruction from Rogen, west-central Sweden, based on blue intensity from tree rings, Holocene, 28, 254–266, https://doi.org/10.1177/0959683617721322, 2018.

Galvan, P., Ponge, J.-F., Chersich, S., and Zanella, A.: Humus Components and Soil Biogenic Structures in Norway Spruce Ecosystems, Soil Sci. Soc. Am. J., 72, 548, https://doi.org/10.2136/sssaj2006.0317, 2008.

Gentili, R., Armiraglio, S., Sgorbati, S., and Baroni, C.: Geomorphological disturbance affects ecological driving forces and plant turnover along an altitudinal stress gradient on alpine slopes, Plant Ecol., 214, 571–586, https://doi.org/10.1007/s11258-013-0190-1, 2013.

Gentili, R., Baroni, C., Panigada, C., Rossini, M., Tagliabue, G., Armiraglio, S., Citterio, S., Carton, A., and Salvatore, M. C.: Glacier shrinkage and slope processes create habitat at high elevation and microrefugia across treeline for alpine plants during warm stages, CATENA, 193, 104626, https://doi.org/10.1016/j.catena.2020.104626, 2020.

Harris, I., Osborn, T. J., Jones, P., and Lister, D.: Version 4 of the CRU TS monthly high-resolution gridded multivariate climate dataset, Sci. Data, 7, 109, https://doi.org/10.1038/s41597-020-0453-3, 2020.

Heeter, K. J., Harley, G. L., Maxwell, J. T., McGee, J. H., and Matheus, T. J.: Late summer temperature variability for the Southern Rocky Mountains (USA) since 1735 CE: applying blue light intensity to low-latitude Picea engelmannii Parry ex Engelm, Clim. Change, 162, 965–988, https://doi.org/10.1007/s10584-020-02772-9, 2020.

Helama, S., Melvin, T. M., and Briffa, K. R.: Regional curve standardization: State of the art, Holocene, 27, 172–177, https://doi.org/10.1177/0959683616652709, 2017.

IPCC: Summary for policymakers, in: Climate Change 2013: The Physical Science Basis. Contribution of Working Group I to the Fifth Assessment Report of the Intergovernmental Panel on Climate Change, edited by: Stocker, T. F., Qin, D., Plattner, G.-K., Tignor, M., Allen, S. K., Boschung, J., Nauels, A., Xia, Y., Bex, V., and Midgley, P. M., Cambridge University Press, Cambridge, United Kingdom and New York, NY, US, 1–28, 2013.

IPCC: Summary for Policymakers, in: Global warming of 1.5°C. An IPCC Special Report on the impacts of global warming of 1.5°C above pre-industrial levels and related global greenhouse gas emission pathways, in the context of strengthening the global response to the threat of climate change, edited by: Masson-Delmotte, V., Zhai, P., Pörtner, H. O., Roberts, D., Skea, J., Shukla, P. R., Pirani, A., Moufouma-Okia, W., Péan, C., Pidcock, R., Connors, S., Matthews, J. B. R., Chen, Y., Zhou, X., Gomis, M. I., Lonnoy, E., Maycock, T., Tignor, M., and Waterfield, T., World Meteorological Organization, Geneva, Switzerland, 32, 2018.

IPCC: Summary for Policymakers, in: The Ocean and Cryosphere in a Changing Climate, edited by: Pörtner, H.-O., Roberts, D. C., Masson-Delmotte, V., Zhai, P., Tignor, M., Poloczanska, E., Mintenbeck, K., Alegría, A., Nicolai, M., Okem, A., Petzold, J., Rama, B., and Weyer, N. M., Cambridge University Press, Cambridge, UK and New York, NY, USA, 3–35, https://doi.org/10.1017/9781009157964.001, ~~2019a~~2019.

IPCC: Summary for Policymakers, in: Climate Change and Land: an IPCC special report on climate change, desertification,

land degradation, sustainable land management, food security, and greenhouse gas fluxes in terrestrial ecosystems, edited by: Shukla, P. R., Skea, J., Buendia Calvo, E., Masson-Delmotte, V., Pörtner, H.-O., Roberts, D. C., Zhai, P., Slade, R., Connors, S., van Diemen, R., Ferrat, M., Haughey, E., Luz, S., Neogi, S., Pathak, M., Petzold, J., Portugal Pereira, J., Vyas, P., Huntley, E., Kissick, K., Belkacemi, M., and Malley, J., Cambridge University Press, Cambridge, UK and New York, NY, USA, 1–36, https://doi.org/10.1017/9781009157988.001, ~~2019b~~2022.

IPCC: Summary for Policymakers, in: Climate Change 2022 – Impacts, Adaptation and Vulnerability, edited by: Pörtner, H.-O., Roberts, D. C., Poloczanska, E. S., Mintenbeck, K., Tignor, M., Alegría, A., Craig, M., Langsdorf, S., Löschke, S., Möller, V., and Okem, A., Cambridge University Press, Cambridge, UK and New York, NY, USA, 3–34, https://doi.org/10.1017/9781009325844.001, 2023.

Isotta, F. A., Frei, C., Weilguni, V., Perčec Tadić, M., Lassègues, P., Rudolf, B., Pavan, V., Cacciamani, C., Antolini, G., Ratto, S. M., Munari, M., Micheletti, S., Bonati, V., Lussana, C., Ronchi, C., Panettieri, E., Marigo, G., and Vertačnik, G.: The climate of daily precipitation in the Alps: Development and analysis of a high-resolution grid dataset from pan-Alpine rain-gauge data, Int. J. Climatol., 34, 1657–1675, https://doi.org/10.1002/joc.3794, 2014.

IUSS Working Group: Technical Report 103, World Soil Resources Reports, Rome, 2007.

Kaczka, R. J., Spyt, B., Janecka, K., Beil, I., Büntgen, U., Scharnweber, T., Nievergelt, D., and Wilmking, M.: Different maximum latewood density and blue intensity measurements techniques reveal similar results, Dendrochronologia, 49, 94–101, https://doi.org/10.1016/j.dendro.2018.03.005, 2018.

Lê, S., Josse, J., and Husson, F.: FactoMineR : An R Package for Multivariate Analysis, J. Stat. Softw., 25, 253–258, https://doi.org/10.18637/jss.v025.i01, 2008.

Leavitt, S. W. and Roden, J.: Stable Isotopes in Tree Rings, edited by: Siegwolf, R. T. W., Brooks, J. R., Roden, J., and Saurer, M., Springer International Publishing, Cham, 3–20 pp., https://doi.org/10.1007/978-3-030-92698-4, 2022.

Leonelli, G., Pelfini, M., D'Arrigo, R. D., Haeberli, W., and Cherubini, P.: Non-stationary Responses of Tree-Ring Chronologies and Glacier Mass Balance to Climate in the European Alps, Arctic, Antarct. Alp. Res., 43, 56–65, https://doi.org/10.1657/1938-4246-43.1.56, 2011.

Leonelli, G., Coppola, A., Baroni, C., Salvatore, M. C., Maugeri, M., Brunetti, M., and Pelfini, M.: Multispecies dendroclimatic reconstructions of summer temperature in the European Alps enhanced by trees highly sensitive to temperature, Clim. Change, 137, 275–291, https://doi.org/10.1007/s10584-016-1658-5, 2016.

Ljungqvist, F. C., Thejll, P., Björklund, J., Gunnarson, B. E., Piermattei, A., Rydval, M., Seftigen, K., Støve, B., and Büntgen, U.: Assessing non-linearity in European temperature-sensitive tree-ring data, Dendrochronologia, 59, 125652, https://doi.org/10.1016/j.dendro.2019.125652, 2020.

Marazzi, S.: Atlante orografico delle Alpi: SOIUSA : suddivisione orografica internazionale unificata del sistema alpino, Priuli & Verlucca, 416 pp., 2005.

McCarroll, D., Pettigrew, E., and Luckman, A.: Blue Reflectance Provides a Surrogate for Latewood Density of High-Latitude Pine Tree Rings Reflectance Provides a Surrogate for Latewood of High-latitude Density Pine Tree Rings, Arctic, Antarct.

Alp. Res., 34, 450–453, 2002.

McPartland, M. Y., St. George, S., Pederson, G. T., and Anchukaitis, K. J.: Does signal-free detrending increase chronology coherence in large tree-ring networks?, Dendrochronologia, 63, 125755, https://doi.org/10.1016/j.dendro.2020.125755, 2020.

Melvin, T. M.: Historical Growth Rates and Changing Climatic Sensitivity of Boreal Conifers, PhD dissertation, University of East Anglia, 271 pp., 2004.

Melvin, T. M. and Briffa, K. R.: A "signal-free" approach to dendroclimatic standardisation, Dendrochronologia, 26, 71–86, https://doi.org/10.1016/j.dendro.2007.12.001, 2008.

Mitchell, T. D. and Jones, P. D.: An improved method of constructing a database of monthly climate observations and associated high-resolution grids, Int. J. Climatol., 25, 693–712, https://doi.org/10.1002/joc.1181, 2005.

New, M., Hulme, M., and Jones, P. D.: Representing Twentieth-Century Space–Time Climate Variability. Part II: Development of 1901–96 Monthly Grids of Terrestrial Surface Climate, J. Clim., 13, 2217–2238, https://doi.org/10.1175/1520-0442(2000)013<2217:RTCSTC>2.0.CO;2, 2000.

Nicolussi, K., Österreicher, A., Weber, G., Leuenberger, M., Bauer, A., and Vogeleit, T.: Blue intensity analyses on spruce, larch and cembran pine cores of living trees from the Alps, in: EuroDendro 2015-Book of Abstracts, 139–140, 2015.

Ols, C., Klesse, S., Girardin, M. P., Evans, M. E. K., DeRose, R. J., and Trouet, V.: Detrending climate data prior to climate–growth analyses in dendroecology: A common best practice?, Dendrochronologia, 79, https://doi.org/10.1016/j.dendro.2023.126094, 2023.

Österreicher, A., Weber, G., Leuenberger, M., and Nicolussi, K.: Exploring blue intensity - comparison of blue intensity and MXD data from Alpine spruce trees, Sci. Tech. Rep., 56–61, https://doi.org/10.2312/GFZ.b103-15069, 2014.

Pepin, N., Bradley, R. S., Diaz, H. F., Baraer, M., Caceres, E. B., Forsythe, N., Fowler, H., Greenwood, G., Hashmi, M. Z., Liu, X. D., Miller, J. R., Ning, L., Ohmura, A., Palazzi, E., Rangwala, I., Schöner, W., Severskiy, I., Shahgedanova, M., Wang, M. B., Williamson, S. N., and Yang, D. Q.: Elevation-dependent warming in mountain regions of the world, Nat. Clim. Chang., 5, 424–430, https://doi.org/10.1038/nclimate2563, 2015.

R Core Team: R: A Language and Environment for Statistical Computing~~. R Foundation for Statistical Computing, Vienna, Austria. https://www.R-project.org/,~~ https://www.r-project.org/, ~~2022~~2024.

Reid, E. and Wilson, R.: Delta blue intensity vs. maximum density: A case study using Pinus uncinata in the Pyrenees, Dendrochronologia, 61, 125706, https://doi.org/10.1016/j.dendro.2020.125706, 2020.

Rydval, M., Larsson, L. Å., McGlynn, L., Gunnarson, B. E., Loader, N. J., Young, G. H. F., and Wilson, R.: Blue intensity for dendroclimatology: Should we have the blues? Experiments from Scotland, Dendrochronologia, 32, 191–204, https://doi.org/10.1016/j.dendro.2014.04.003, 2014.

Rydval, M., Gunnarson, B. E., Loader, N. J., Cook, E. R., Druckenbrod, D. L., and Wilson, R.: Spatial reconstruction of Scottish summer temperatures from tree rings, Int. J. Climatol., 37, 1540–1556, https://doi.org/10.1002/joc.4796, 2016.

Salvatore, M. C., Zanoner, T., Baroni, C., Carton, A., Banchieri, F. A., Viani, C., Giardino, M., and Perotti, L.: The state of Italian glaciers: A snapshot of the 2006-2007 hydrological period, Geogr. Fis. e Din. Quat., 38, 175–198,

https://doi.org/10.4461/GFDQ.2015.38.16, 2015.

Saulnier, M., Corona, C., Stoffel, M., Guibal, F., and Edouard, J.-L.: Climate-growth relationships in a Larix decidua Mill. network in the French Alps, Sci. Total Environ., 664, 554–566, https://doi.org/10.1016/j.scitotenv.2019.01.404, 2019.

Schwab, N., Kaczka, R. J., Janecka, K., Böhner, J., Chaudhary, R., Scholten, T., and Schickhoff, U.: Climate Change-Induced Shift of Tree Growth Sensitivity at a Central Himalayan Treeline Ecotone, Forests, 9, 267, https://doi.org/10.3390/f9050267, 2018.

Schweingruber, F. H.: Tree Rings Basic and Applications of Dendrochronology, Springer Netherlands, Dordrecht, 276 pp., https://doi.org/10.1007/978-94-009-1273-1, 1988.

Seftigen, K., Fuentes, M., Ljungqvist, F. C., and Björklund, J.: Using Blue Intensity from drought-sensitive Pinus sylvestris in Fennoscandia to improve reconstruction of past hydroclimate variability, Clim. Dyn., 55, 579–594, https://doi.org/10.1007/s00382-020-05287-2, 2020.

Seftigen, K., Fonti, M. V., Luckman, B., Rydval, M., Stridbeck, P., von Arx, G., Wilson, R., and Björklund, J.: Prospects for dendroanatomy in paleoclimatology – a case study on Picea engelmannii from the Canadian Rockies, Clim. Past, 18, 1151–1168, https://doi.org/10.5194/cp-18-1151-2022, 2022.

Sheppard, P. R. and Wiedenhoeft, A.: An advancement in removing extraneous color from wood for low-magnification reflected-light image analysis of conifer tree rings, Wood Fiber Sci., 39, 173–183, 2007.

Solomina, O. N., Bushueva, I., Dolgova, E., Jomelli, V., Alexandrin, M., Mikhalenko, V., and Matskovsky, V. V.: Glacier variations in the Northern Caucasus compared to climatic reconstructions over the past millennium, Glob. Planet. Change, 140, 28–58, https://doi.org/10.1016/j.gloplacha.2016.02.008, 2016.

Trachsel, M., Kamenik, C., Grosjean, M., McCarroll, D., Moberg, A., Brázdil, R., Büntgen, U., Dobrovolný, P., Esper, J., Frank, D. C., Friedrich, M., Glaser, R., Larocque-Tobler, I., Nicolussi, K., and Riemann, D.: Multi-archive summer temperature reconstruction for the European Alps, AD 1053-1996, Quat. Sci. Rev., 46, 66–79, https://doi.org/10.1016/j.quascirev.2012.04.021, 2012.

Tsvetanov, N., Dolgova, E., and Panayotov, M.: First measurements of Blue intensity from Pinus peuce and Pinus heldreichii tree rings and potential for climate reconstructions, Dendrochronologia, 60, 125681, https://doi.org/10.1016/j.dendro.2020.125681, 2020.

Turchin, P., Wood, S. N., Ellner, S. P., Kendall, B. E., Murdoch, W. W., Fischlin, A., Casas, J., McCauley, E., and Briggs, C. J.: Dynamical effects of plant quality and parasitism on population cycles of larch budmoth, Ecology, 84, 1207–1214, https://doi.org/10.1890/0012-9658(2003)084[1207:DEOPQA]2.0.CO;2, 2003.

Unterholzner, L., Castagneri, D., Cerrato, R., Știrbu, M., Roibu, C.-C., and Carrer, M.: Climate response of a glacial relict conifer across its distribution range is invariant in space but not in time, Sci. Total Environ., 906, 167512, https://doi.org/10.1016/j.scitotenv.2023.167512, 2024.

Wilmking, M., van der Maaten-Theunissen, M., van der Maaten, E., Scharnweber, T., Buras, A., Biermann, C., Gurskaya, M., Hallinger, M., Lange, J., Shetti, R., Smiljanic, M., and Trouillier, M.: Global assessment of relationships between climate and

tree growth, Glob. Chang. Biol., 26, 3212–3220, https://doi.org/10.1111/gcb.15057, 2020.

Wilson, R., Rao, R., Rydval, M., Wood, C. V., Larsson, L. Å., and Luckman, B. H.: Blue Intensity for dendroclimatology: The BC blues: A case study from British Columbia, Canada, Holocene, 24, 1428–1438, https://doi.org/10.1177/0959683614544051, 2014.

Wilson, R., Anchukaitis, K. J., Briffa, K. R., Büntgen, U., Cook, E. R., D'Arrigo, R. D., Davi, N., Esper, J., Frank, D. C., Gunnarson, B. E., Hegerl, G., Helama, S., Klesse, S., Krusic, P. J., Linderholm, H. W., Myglan, V. S., Osborn, T. J., Rydval, M., Schneider, L., Schurer, A., Wiles, G. C., Zhang, P., and Zorita, E.: Last millennium northern hemisphere summer temperatures from tree rings: Part I: The long term context, Quat. Sci. Rev., 134, 1–18, https://doi.org/10.1016/j.quascirev.2015.12.005, 2016.

Wilson, R., D'Arrigo, R., Andreu-Hayles, L., Oelkers, R., Wiles, G., Anchukaitis, K., and Davi, N.: Experiments based on blue intensity for reconstructing North Pacific temperatures along the Gulf of Alaska, Clim. Past, 13, 1007–1022, https://doi.org/10.5194/cp-13-1007-2017, 2017a.

Wilson, R., Wilson, D., Rydval, M., Crone, A., Büntgen, U., Clark, S., Ehmer, J., Forbes, E., Fuentes, M., Gunnarson, B. E., Linderholm, H. W., Nicolussi, K., Wood, C. V., and Mills, C.: Facilitating tree-ring dating of historic conifer timbers using Blue Intensity, J. Archaeol. Sci., 78, 99–111, https://doi.org/10.1016/j.jas.2016.11.011, 2017b.

Wilson, R., Anchukaitis, K. J., Andreu-Hayles, L., Cook, E. R., D'Arrigo, R. D., Davi, N., Haberbauer, L., Krusic, P. J., Luckman, B., Morimoto, D., Oelkers, R., Wiles, G., and Wood, C. V.: Improved dendroclimatic calibration using blue intensity in the southern Yukon, The Holocene, 29, 1817–1830, https://doi.org/10.1177/0959683619862037, 2019.

Wilson, R., Allen, K., Baker, P., Boswijk, G., Buckley, B., Cook, E., D'arrigo, R., Druckenbrod, D., Fowler, A., Grandjean, M., Krusic, P., and Palmer, J.: Evaluating the dendroclimatological potential of blue intensity on multiple conifer species from Tasmania and New Zealand, Biogeosciences, 18, 6393–6421, https://doi.org/10.5194/bg-18-6393-2021, 2021.

Zang, C. and Biondi, F.: treeclim: an R package for the numerical calibration of proxy-climate relationships, Ecography (Cop.)., 38, 431–436, https://doi.org/10.1111/ecog.01335, 2015.

Zemp, M., Frey, H., Gärtner-Roer, I., Nussbaumer, S. U., Hoelzle, M., Paul, F., Haeberli, W., Denzinger, F., Ahlstrøm, A. P., Anderson, B. M., Bajracharya, S., Baroni, C., Braun, L. N., Cáceres, B. E., Casassa, G., Cobos, G., Dávila, L. R., Delgado Granados, H., Demuth, M. N., Espizua, L., Fischer, A., Fujita, K., Gadek, B., Ghazanfar, A., Ove Hagen, J., Holmlund, P., Karimi, N., Li, Z., Pelto, M., Pitte, P., Popovnin, V. V., Portocarrero, C. A., Prinz, R., Sangewar, C. V., Severskiy, I., Sigurđsson, O., Soruco, A., Usubaliev, R., and Vincent, C.: Historically unprecedented global glacier decline in the early 21st century, J. Glaciol., 61, 745–762, https://doi.org/10.3189/2015JoG15J017, 2015.